

AEDC-TR-80-45

C.1

**ARCHIVE COPY
DO NOT LOAN**



Infrared Standards to Improve Chamber 7V Beam Irradiance Calibrations

F. G. Sherrell
ARO, Inc.

January 1981

Final Report for Period October 1, 1979 – September 30, 1980

Approved for public release; distribution unlimited.

**TECHNICAL REPORTS
FILE COPY**

PROPERTY OF U.S. AIR FORCE
AEDC TECHNICAL LIBRARY

Property of U. S. Air Force
AEDC LIBRARY
F40600-81-C-0004

AEDC TECHNICAL LIBRARY



5 0720 00034 6280

**ARNOLD ENGINEERING DEVELOPMENT CENTER
ARNOLD AIR FORCE STATION, TENNESSEE
AIR FORCE SYSTEMS COMMAND
UNITED STATES AIR FORCE**

NOTICES

When U. S. Government drawings, specifications, or other data are used for any purpose other than a definitely related Government procurement operation, the Government thereby incurs no responsibility nor any obligation whatsoever, and the fact that the Government may have formulated, furnished, or in any way supplied the said drawings, specifications, or other data, is not to be regarded by implication or otherwise, or in any manner licensing the holder or any other person or corporation, or conveying any rights or permission to manufacture, use, or sell any patented invention that may in any way be related thereto.

Qualified users may obtain copies of this report from the Defense Technical Information Center.

References to named commercial products in this report are not to be considered in any sense as an indorsement of the product by the United States Air Force or the Government.

This report has been reviewed by the Office of Public Affairs (PA) and is releasable to the National Technical Information Service (NTIS). At NTIS, it will be available to the general public, including foreign nations.

APPROVAL STATEMENT


This report has been reviewed and approved.



MARSHALL K. KINGERY
Project Manager
Directorate of Technology

Approved for publication:

FOR THE COMMANDER



MARION L. LASTER
Director of Technology
Deputy for Operations

UNCLASSIFIED

| REPORT DOCUMENTATION PAGE | | READ INSTRUCTIONS BEFORE COMPLETING FORM |
|---|----------------------|---|
| 1 REPORT NUMBER AEDC-TR-80-45 | 2 GOVT ACCESSION NO. | 3 RECIPIENT'S CATALOG NUMBER |
| 4 TITLE (and Subtitle) INFRARED STANDARDS TO IMPROVE CHAMBER 7V BEAM IRRADIANCE CALIBRATIONS | | 5 TYPE OF REPORT & PERIOD COVERED Final Report, Oct. 1, 1979 - Sept. 30, 1980 |
| | | 6 PERFORMING ORG. REPORT NUMBER |
| 7 AUTHOR(s) F. G. Sherrell, ARO, Inc., a Sverdrup Corporation Company | | 8 CONTRACT OR GRANT NUMBER(s) |
| 9 PERFORMING ORGANIZATION NAME AND ADDRESS Arnold Engineering Development Center/DOT Air Force Systems Command Arnold Air Force Station, Tennessee 37389 | | 10 PROGRAM ELEMENT PROJECT TASK AREA & WORK UNIT NUMBERS Program Element 65807F |
| 11 CONTROLLING OFFICE NAME AND ADDRESS Arnold Engineering Development Center/DOS Air Force Systems Command Arnold Air Force Station, Tennessee 37389 | | 12 REPORT DATE January 1981 |
| | | 13 NUMBER OF PAGES 49 |
| 14 MONITORING AGENCY NAME & ADDRESS (if different from Controlling Office) | | 15 SECURITY CLASS. (of this report) UNCLASSIFIED |
| | | 15a DECLASSIFICATION/DOWNGRADING SCHEDULE N/A |
| 16 DISTRIBUTION STATEMENT (of this Report) Approved for public release; distribution unlimited. | | |
| 17 DISTRIBUTION STATEMENT (of the abstract entered in Block 20, if different from Report) | | |
| 18 SUPPLEMENTARY NOTES Available in Defense Technical Information Center (DTIC). | | |
| 19 KEY WORDS (Continue on reverse side if necessary and identify by block number); infrared detection high vacuum bolometers thermistors calibration low temperature blackbody radiation vacuum chambers | | |
| 20 ABSTRACT (Continue on reverse side if necessary and identify by block number) A working standard, low-temperature, blackbody has been developed for use in establishing radiometric calibrations that are directly traceable to the National Bureau of Standards. The blackbody will be used in the process of establishing a calibration of the 7V beam irradiance, as required for LWIR sensor testing. The 7V beam irradiance calibration process is reviewed to indicate the manner in which the working standard blackbody fits into the | | |

UNCLASSIFIED

UNCLASSIFIED

20. ABSTRACT (Continued)

overall calibration scheme. A complete description of the design and calibration of the working standard blackbody is presented. The device is utilized to calibrate a phosphorous-doped, silicon bolometer and the bolometer calibration procedure and results, are also presented. In the overall 7V beam irradiance calibration process, the bolometer will be used to calibrate the operational sources that are utilized in 7V sensor test installations.

UNCLASSIFIED

PREFACE

The work reported herein was conducted by the Arnold Engineering Development Center (AEDC), Air Force Systems Command (AFSC). The Air Force project manager was Mr. Marshall Kingery. The results of the research presented were obtained by ARO, Inc., AEDC Group (a Sverdrup Corporation Company), operating contractor for the AEDC, AFSC, Arnold Air Force Station, Tennessee, under ARO Project Number V32K-12A. The manuscript was submitted for publication on September 4, 1980.

CONTENTS

| | <u>Page</u> |
|--|-------------|
| 1.0 INTRODUCTION | 5 |
| 2.0 REVIEW OF THE 7V INFRARED SOURCES AND CALIBRATION DEVICES | 6 |
| 3.0 DESCRIPTION OF THE VKF STANDARD INFRARED SOURCE | |
| 3.1 Source Unit Design | 15 |
| 3.2 Cavity Temperature Measurement and Control System | 20 |
| 3.3 Summary of the National Bureau of Standards Calibration Results | 24 |
| 4.0 BOLOMETER CALIBRATION PROCEDURE AND RESULTS | 24 |
| 5.0 SUMMARY | 32 |
| REFERENCES | 32 |

ILLUSTRATIONS

Figure

| | |
|---|----|
| 1. Schematic of the Aerospace Chamber (7V) | 5 |
| 2. Cross-Sectional View of a Triple Integrating Sphere Infrared Source | 7 |
| 3. Schematic of Radiation Monitor Telescope | 9 |
| 4. Photograph of Radiation Monitor Telescope | 10 |
| 5. Chopper in Radiation Monitor Telescope | 10 |
| 6. Filter Wheel in Radiation Monitor Telescope | 11 |
| 7. Reference Blackbody in Radiation Monitor Telescope | 11 |
| 8. Chamber for Infrared Source Testing | 13 |
| 9. Molelectron Bolometer | 14 |
| 10. AEDC-VKF Standard Infrared Source, Cross-Sectional View | 16 |
| 11. AEDC-VKF Standard Infrared Source Components | 17 |
| 12. Schematic for Analysis of Blackbody Radiant Output | 18 |
| 13. Block Diagram of AEDC-VKF Standard Infrared Source Control System | 21 |
| 14. Photograph of AEDC-VKF Standard Infrared Source Control Panel | 22 |
| 15. Performance Testing Assembly | 25 |
| 16. Test Chamber Installation | 26 |
| 17. Bolometer Instrumentation System Schematic | 28 |

TABLES

| | <u>Page</u> |
|---|-------------|
| 1. Thermistor Calibration Data | 23 |
| 2. Experimental Results of Calibration of the Bolometer System with the SIRS | 30 |
| 3. Summary of Bolometer System Responsivity Calibrations | 31 |

APPENDIX

| | |
|-----------------------------|----|
| REPORT OF CALIBRATION | 35 |
| NOMENCLATURE | 49 |

1.0 INTRODUCTION

The von Kármán Gas Dynamics Facility (VKF) Aerospace Chamber (7V) at the Arnold Engineering Development Center (AEDC) is equipped to test long wavelength infrared (LWIR) sensors. The chamber is a 7-ft-diam by 12-ft-long, high-vacuum vessel containing a light-tight, 20°K liner. The infrared target simulator consists, basically, of a pinhole (nominal 300°K) radiation source located at the focal point of a 28-in-diam spherical collimating mirror. The focal length of the mirror is 105.3 in. All hardware in the chamber is cooled to 20°K during sensor testing. A schematic of the system is shown in Fig. 1.

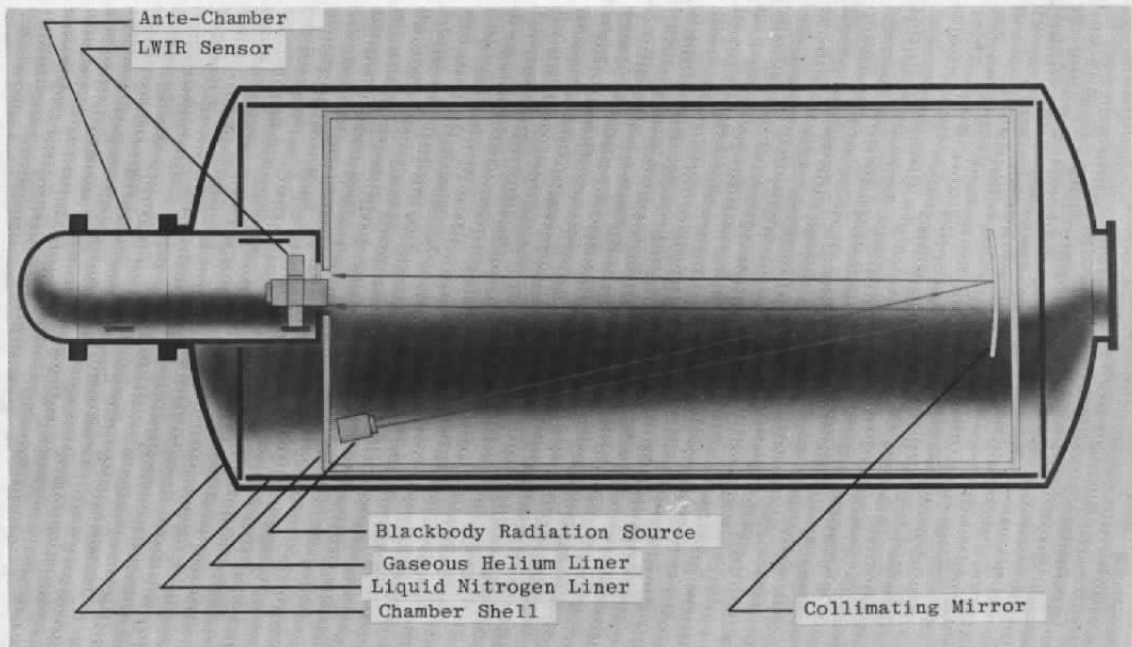


Figure 1. Schematic of the Aerospace Chamber (7V).

With this target simulator design, the point source appears to be at infinity when observed back "through" the collimating mirror.

The 28-in.-diam beam reflected from the collimating mirror overfills the input aperture of the typical test sensor, and apparent target motion in the horizontal plane is generated by mechanically rotating the mirror about an axis perpendicular to the plane of Fig. 1. Apparent motion in the vertical plane is generated by mechanically translating the pinhole radiation source perpendicular to Fig. 1. These apparent target motions provide the means for sensor focal-plane mapping and for responsivity calibrations of individual detector elements on the focal plane.

During the past decade, several AEDC projects have been directed toward developing infrared sources for use in the 7V target simulator. In addition, various devices have been developed for calibration of the 7V beam irradiance. All of these projects were complicated by the extremely low irradiance levels required for conducting LWIR sensor tests. Both the generation and calibration of the required irradiance levels were difficult problems. In fact, the required source intensity levels fell below the operating range of the National Bureau of Standards (NBS) facility for calibrating low-temperature blackbodies. Consequently, the process of establishing an NBS-traceable calibration of the 7V beam irradiance has become a complex process involving several operational devices and five calibration transfers. This process is reviewed in Section 2.0, along with brief descriptions of the operational devices involved.

The discussion in Section 2.0 also reviews the need for a working standard infrared source which could serve as the primary device for transferring a radiometric calibration from the NBS to the AEDC. Such a source was developed, and in May 1979, it was shipped to the NBS for a formal radiometric calibration. Section 3.0 describes the source and its electronic control unit in detail. The NBS report of the radiometric calibration is presented in the Appendix.

More recently, the NBS radiometric calibration was transferred to a silicon bolometer using the working standard infrared source as the transfer device. Section 4.0 of this report describes the bolometer calibration procedure and results.

Presently, the bolometer is being applied to the calibration of the operational sources that are actually used in the generation and calibration of the 7V beam irradiance. These calibrations are being performed as a part of the Space Infrared Experiment (SIRE) sensor test, and will be reported later.

2.0 REVIEW OF THE 7V INFRARED SOURCES AND CALIBRATION DEVICES

One of the usual LWIR sensor test requirements is to measure the responsivity (i.e., sensor output signal versus input beam irradiance) over the several orders of magnitude of the sensor's operating range. Because of the extremely low levels of beam irradiance (watt/cm^2), this is a difficult test requirement. The irradiance saturation level for a state-of-the-art, high-performance LWIR sensor is approximately 10^{-10} watt/cm^2 of 300°K Planckian radiation, and the sensor is responsive to irradiance levels below 10^{-16} watt/cm^2 . To meet basic requirements, the radiation source in the 7V target simulator must be designed to allow six or more orders of magnitude of linear adjustment of the 7V beam irradiance.

v

In recent years, infrared integrating spheres have been used as the variable intensity sources in the 7V target simulator (Ref. 1). These sources provide over seven orders of magnitude of irradiance range and, in addition, have other very desirable operational features. Specifically, irradiance levels ranging from below 10^{-18} to above 10^{-11} watt/cm² can be generated with integrating sphere infrared sources without changing the source temperature or the output aperture. Figure 2 is a cross-sectional view of this type of infrared source. The output power radiates from a 0.0256-in.-diam aperture on the center sphere. The spheres are 1.5 in. in diameter and have diffusely reflecting, gold-coated surfaces. High-range power comes from the suspended capsule in the upper sphere, whereas low-range power is injected into the lower sphere by the blackbody cavity. Output intensity is controlled by the capsule and cavity aperture wheels which contain a total of 22 apertures and provide a range of over seven orders of magnitude of output intensity adjustment.

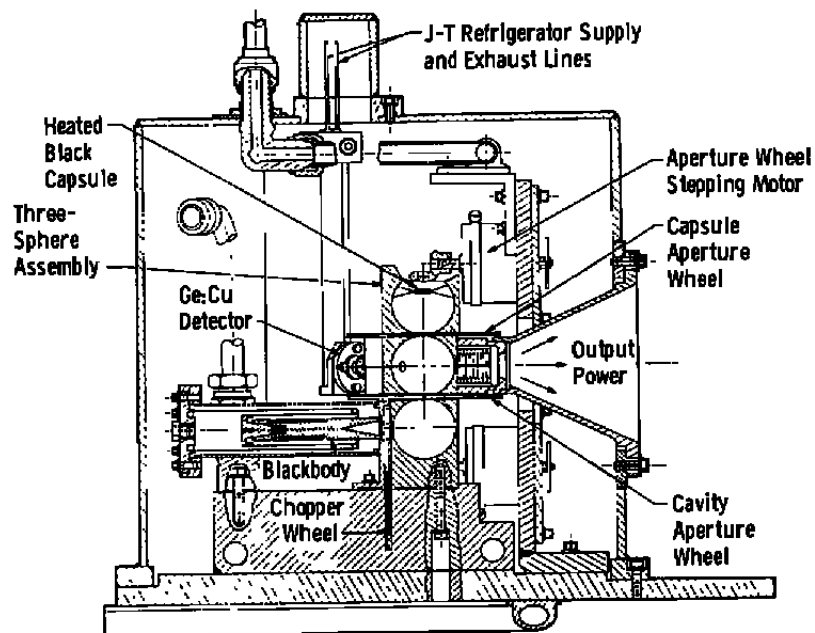


Figure 2. Cross-sectional view of a triple integrating sphere infrared source.

Although the use of integrating sphere devices satisfies some basic test requirements, it also generates a formidable calibration problem. In a typical LWIR sensor test program, the 7V beam irradiance must be calibrated with working standards whose calibrations are traceable to the National Bureau of Standards (NBS). When using integrating sphere infrared sources are used, this calibration is complicated by several factors:

1. There are no generally accepted calibration radiometers of sufficient sensitivity to directly measure and calibrate the 7V beam irradiance in the 10^{-18} to 10^{-11} watt/cm² range.
2. The NBS service for calibrating low-temperature (300°K) blackbodies in a 20°K vacuum environment is for relatively high-intensity levels. Blackbodies which the NBS can presently calibrate generate 7V beam irradiances starting at approximately 10^{-10} watt/cm² and ranging upward.
3. Sources which use integrating spheres are very complex devices, and their output intensities cannot be accurately calculated. Therefore, in spite of (1), the 7V beam irradiance must be directly measured and calibrated to the extent possible by current technology.

Because of these factors, it has become necessary to develop a 7V radiation monitor telescope for use in calibrating the 7V beam irradiance. The device is shown schematically in Fig. 3. Figure 4 is a photograph of the instrument with side and end covers removed, and Figs. 5, 6, and 7 are close-up photographs of various components in the device. These components are identified in Fig. 3. In operation, the device is actively cooled to 20°K, except for the detector, which is cooled to below 5°K by the Joule-Thomson cooler.

The temperature of the heated cavity in the reference blackbody (Item 5, Fig. 3) is adjustable from 200 to 400°K, and the output aperture has a diameter of 0.0256 in. With these characteristics, the output intensity of the reference blackbody is high enough to fall within the operating range of the NBS facility for calibrating low-temperature blackbodies (Ref. 2). Therefore, as will be discussed later, it becomes possible to establish NBS-traceable calibrations of the reference blackbody intensity and, eventually, the 7V beam irradiance.

The detailed procedures for using the radiation monitor telescope in 7V beam irradiance calibrations are still being developed, but the essential steps are as follows:

1. With the 7V beam turned off, turn the reference blackbody (Item 5, Fig. 3) on and set the blackbody cavity temperature to 300°K.
2. Calibrate the detector (Item 7, Fig. 3) with radiation from the reference blackbody.
3. Turn the reference blackbody off and turn the 7V beam on. Set the 7V target temperature to 300°K and center the target image on the telescope detector.

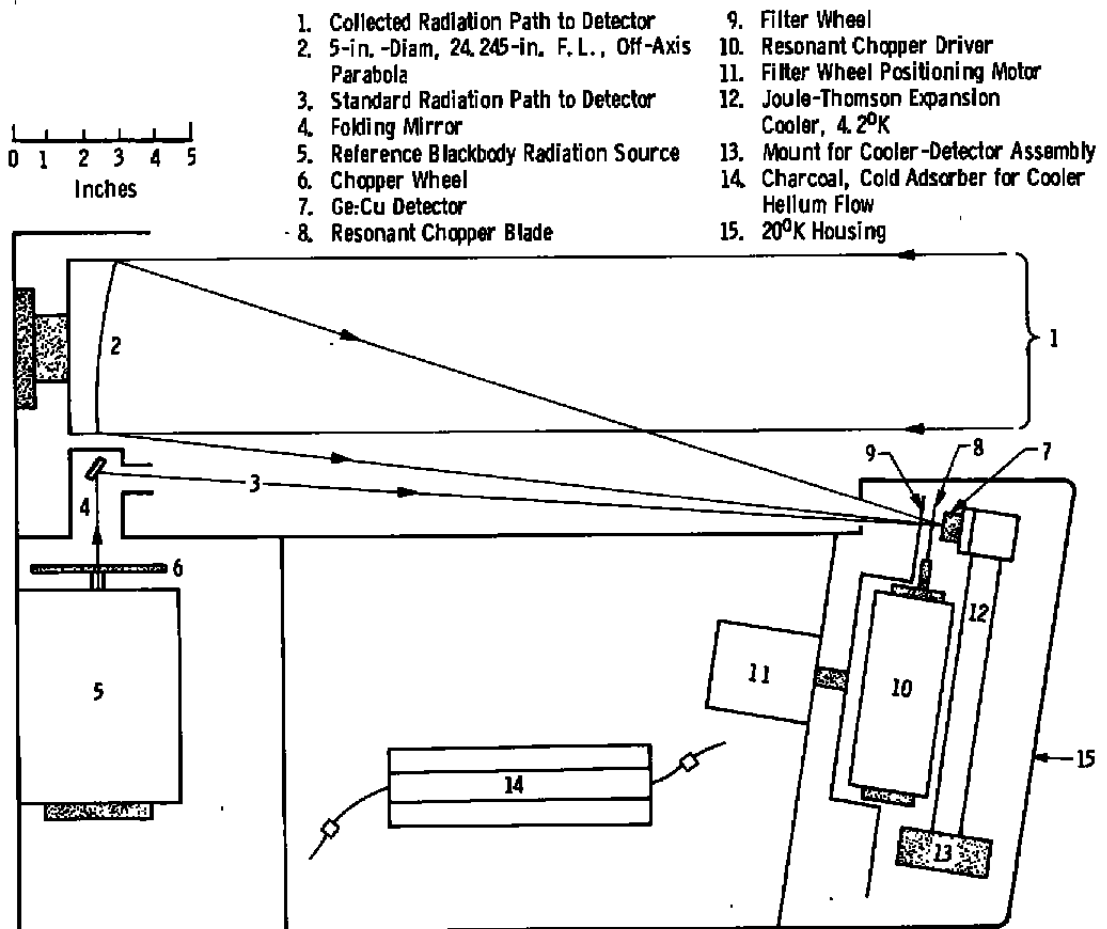


Figure 3. Schematic of radiation monitor telescope.

4. Measure the detector signal generated by the radiant power (Item 1, Fig. 3) that is focused on the detector.
5. Calculate the amount of focused power (watts) by dividing the detector signal from (4) by the responsivity from (2).
6. Calculate the 7V beam irradiance by dividing the power from (5) by the area of the parabolic mirror (Item 2, Fig. 3).

The actual calibration process starts with Step (2), the determination of detector responsivity to 300°K radiant power. This parameter is calculated from an expression of the form

$$\text{Responsivity} = \frac{\text{Detector Output Signal (volts)}}{\text{Reference Blackbody Intensity (watts/sr)} \times \text{Detector Solid Angle (sr)}}$$

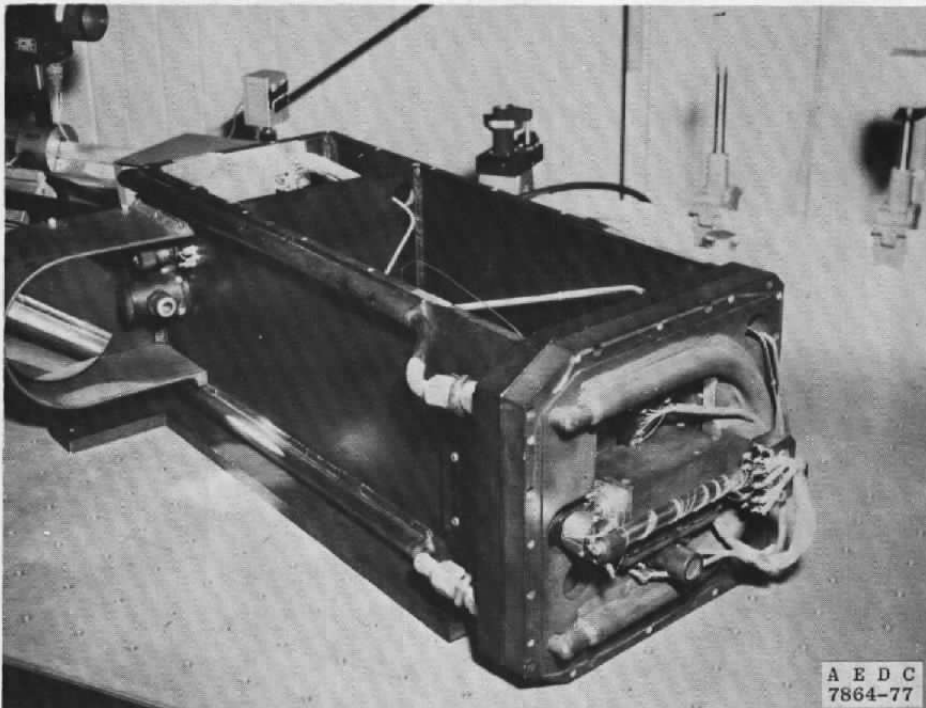


Figure 4. Photograph of radiation monitor telescope.

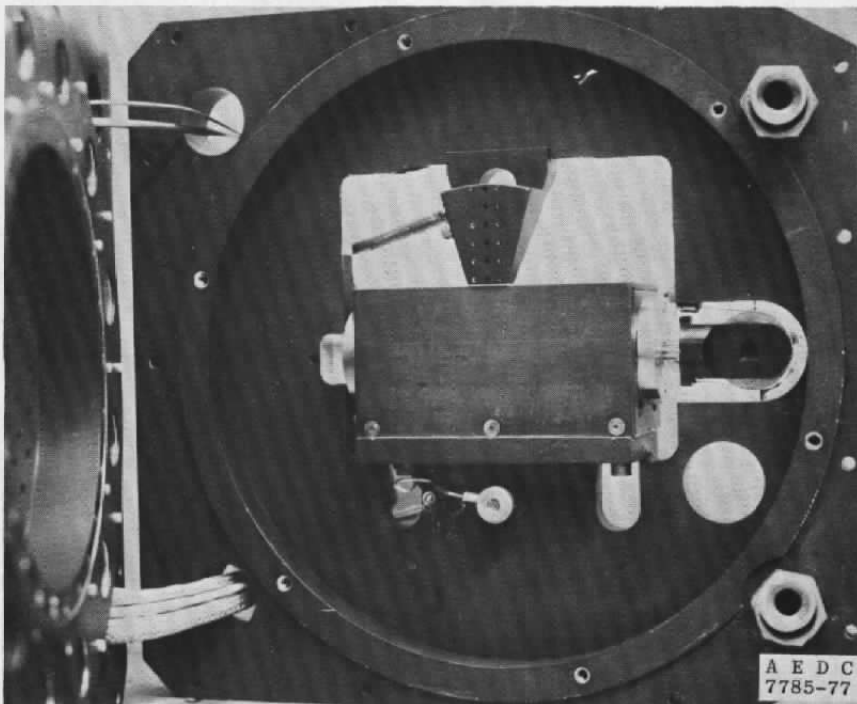


Figure 5. Chopper in radiation monitor telescope.

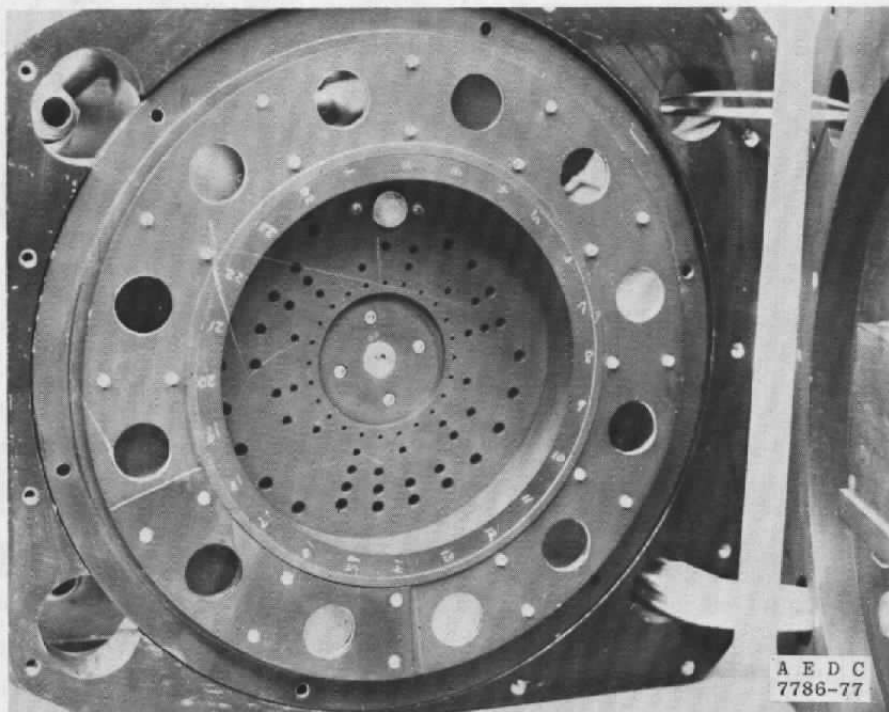


Figure 6. Filter wheel in radiation monitor telescope.

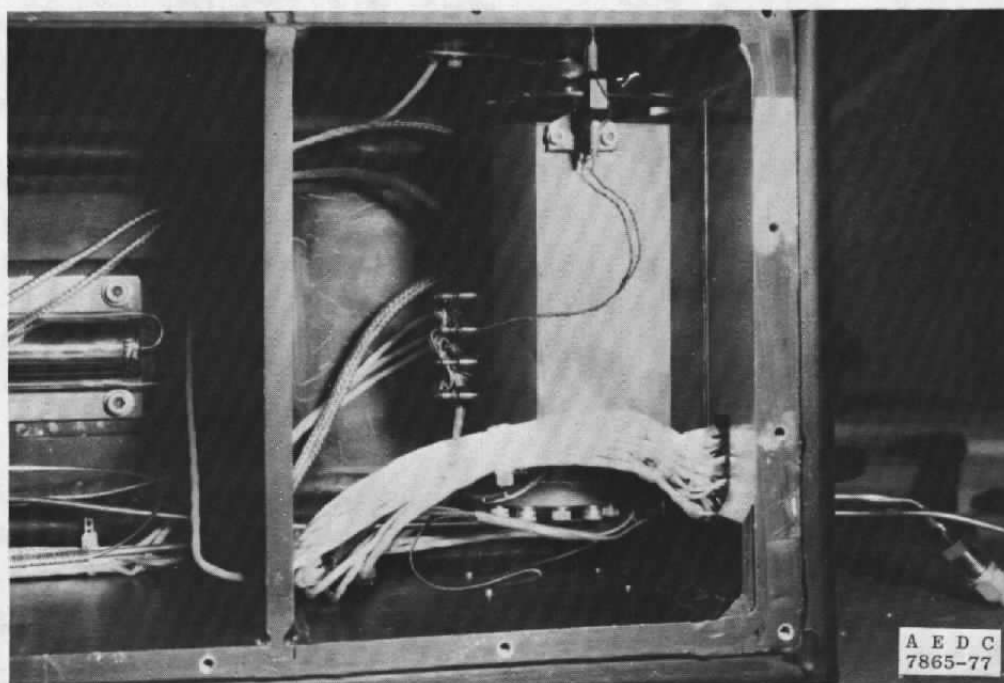


Figure 7. Reference blackbody in radiation monitor telescope.

The detector output signal in this expression is measured with a lock-in amplifier, and the detector solid angle is calculated from the physical dimensions of components in the radiation monitor telescope. However, the determination of the reference blackbody intensity is a formal radiometric calibration process. Therefore, calibration of the 7V beam irradiance requires the initial, basic calibration of a low-temperature blackbody under cryogenic-vacuum conditions. Further, the calibration must be directly traceable to the NBS.

In the past several years, much effort has been directed toward developing the capability to calibrate low-temperature blackbodies at the AEDC. The effort has been successfully completed, and results are presented in this report. The calibration capability at the AEDC is based on the use of a working standard bolometer to directly measure and calibrate the output intensity of infrared sources such as the reference blackbody in the 7V radiation monitor telescope. The blackbody infrared source to be calibrated is temporarily installed in a small high-vacuum research chamber, along with the bolometer. The experimental arrangement is shown in Fig. 8. The infrared source and the bolometer are mounted in a 20°K light-tight liner. A 20°K gaseous-helium (GHe) flow cools both the liner and the infrared source housing. The bolometer is mounted on a liquid-helium (LHe) dewar which is pumped with a 13-cfm rotary pump. This reduces the helium pressure inside the dewar to approximately 4.7 torr and cools the bolometer to its required operating temperature of approximately 1.5°K. At this temperature, the bolometer responsivity is around 6.8×10^5 volts/watt, and the bolometer can be used to measure source intensity levels down to 6×10^{-6} watt/sr, or slightly lower.

The bolometer was developed by Molectron Corp. for the AEDC. Since the bolometer is described in detail in Refs. 3 and 4, only a brief review of its characteristics will be presented. The basic bolometer element is a 5 mm by 5 mm by 0.3 mm silicon chip. Phosphorous was diffused into one face to form a bolometric surface having a very high temperature coefficient of resistivity in the 1.5°K region (Ref. 3). Two leads supplying a $0.25\mu\text{A}$ bias current are connected to this surface. A 780-ohm thin-film Nichrome® heater was vacuum-deposited on the other face, and two leads were connected to supply a heater voltage. The face with the heater was overcoated with black paint to absorb incident radiant energy. This design permits power to be injected either radiometrically or electrically. When power is injected, the change in resistance of the bolometer surface generates a change in the voltage drop across the bolometer surface. This voltage change is measured and calibrated as a function of injected power. Figure 9 is a schematic of the essential bolometer characteristics.

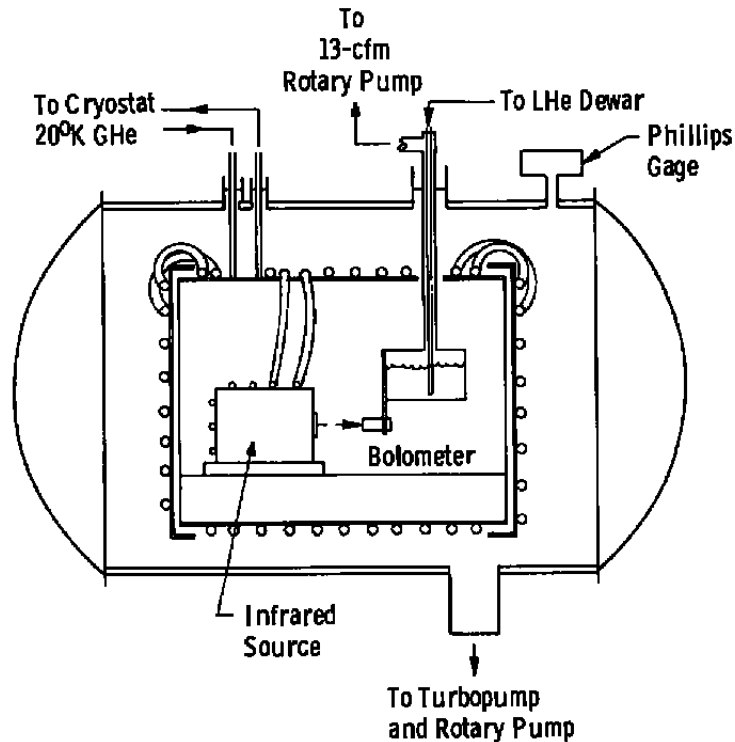
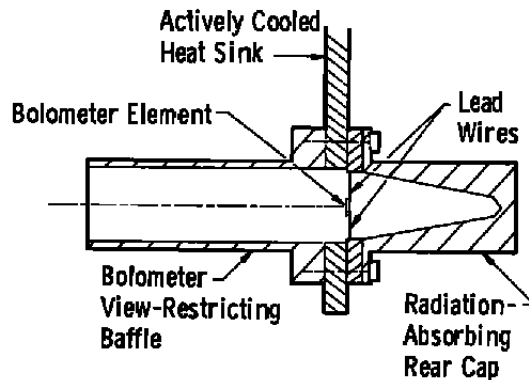


Figure 8. Chamber for infrared source testing.

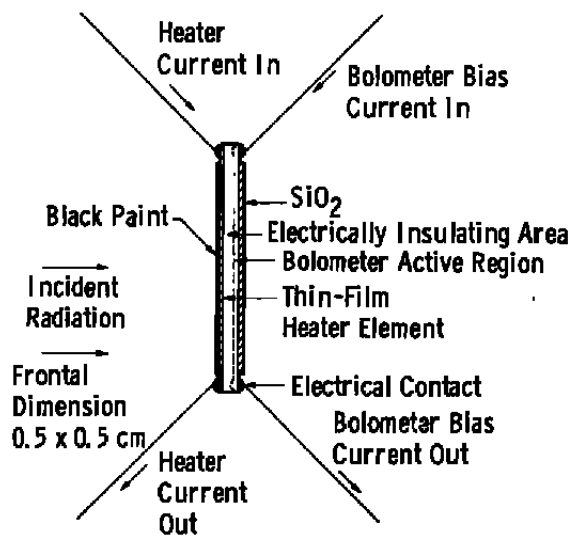
As it was originally designed, the bolometer's response to electrical and radiometric power was intended to be equal. With this feature, the bolometer could first be calibrated with electrical standards and then be used to measure radiant power. Unfortunately, the bolometer was found to be about 20 percent less responsive to heater power than radiant power (Ref. 4). For this reason, it became necessary to develop a working standard blackbody radiation source for radiometric calibration of the bolometer response. Such a source has been developed and sent to the NBS for calibration. The source, referred to as the AEDC-VKF Standard Infrared Source (SIRS), is described in detail in the next section. The NBS report on the source calibration is presented in the Appendix.

After the NBS calibration project was completed, the SIRS was returned to the AEDC and applied to the radiometric calibration of the bolometer response. The bolometer calibration procedures and results are presented in Section 4.0.

The bolometer is presently being used to transfer the NBS calibration to the reference blackbody of the 7V radiation monitor telescope. In the near future, as a requirement of the SIRE Sensor Test Program in the 7V chamber, the 7V radiation monitor telescope will be used to calibrate the 7V beam irradiance.



a. Bolometer mounting



b. Bolometer element cross section
 Figure 9. Molelectron bolometer.

3.0 DESCRIPTION OF THE AEDC-VKF STANDARD INFRARED SOURCE

As indicated previously, the AEDC-VKF Standard Infrared Source (SIRS) was designed and developed specifically for transferring a radiometric calibration from the NBS facilities to the AEDC equipment. In this section, the SIRS will be described in detail, and the results of the NBS calibration project will be discussed. Section 4.0 will report the application of the SIRS to the bolometer calibration.

3.1 SOURCE UNIT DESIGN

A cross-sectional view of the SIRS is shown in Fig. 10, and Fig. 11 shows the unit in a partially assembled state. The heater core material is aluminum, which was anodized to provide electrical insulation for the 0.005-in. platinum wire heater. The anodized aluminum heater core cap is threaded to screw onto the heater core. All surfaces showing inside the blackbody cavity were painted with 3M Nextel® Velvet before the core cap was installed. Silver-filled epoxy was used as a thread dope to ensure an effective thermal bond between the core and cap. The outside surface of the cap was polished to decrease the radiant emittance from the exterior surface and to help control stray radiation. The platinum wire heater winding was secured with fiberglass string which was vacuum-impregnated with an application of high-temperature (600°F) red silicone rubber. Finally, the heater core was wrapped with aluminum foil to further reduce the radiant emittance from the exterior surface.

Thermal isolation and mechanical support of the heater core are accomplished by use of low-conductivity, thin-wall stainless-steel tubing. As indicated in Fig. 10, two counter-mounted pieces of stainless-steel tubing connect the core mounting stud to the 20°K mounting flange. Additional thermal isolation of the core is provided by the high vacuum that is maintained inside the source housing during normal operations. The total power required to maintain the core at 300°K, with the housing at 20°K, is approximately 1.2 watts.

Two core temperature sensors are bonded into the deep insertion holes with a high-temperature epoxy (Tra-Bond 2211®). The two sensors are miniature, high-resolution thermistors which were first epoxied to the end of short pieces of four-hole ceramic tubing. A conventional four-lead hookup was used in the thermistors, with the four leads on each thermistor being brought out through the holes in the ceramic tubing. This assembly was then bonded with epoxy into the insertion holes shown in Fig. 10. More information on the thermistors is presented in Sections 3.2 and 3.3.

Total emittance of the blackbody cavity in the heater core was calculated by the method of Gouffe, summarized in Ref. 5, and was found to be 0.9998. Therefore, for all practical purposes, the cavity emittance may be assumed to be unity.

The design of the elements involved in extracting the radiative output from the heated cavity is somewhat unconventional and is aimed at eliminating both stray light and output aperture heating. Specifically, a black, cold (20°K) cavity is established between the output aperture and the heater core (Fig. 10). The cavity is formed by the truncated conical cuts in the radiation shielding disk and in the output aperture mounting disk (Fig. 11). This cavity

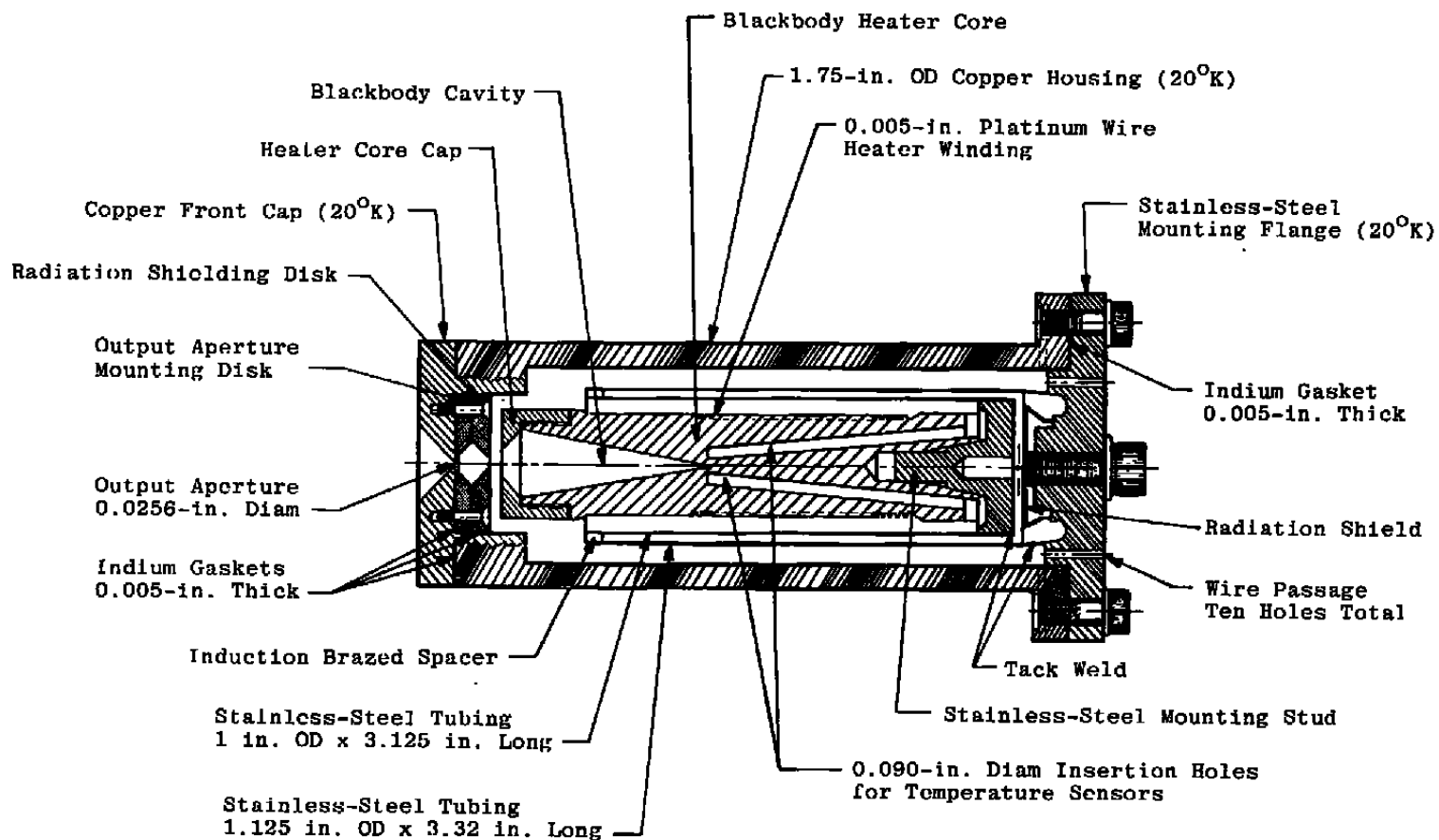


Figure 10. AEDC-VKF standard infrared source, cross-sectional view.



Figure 11. AEDC-VKF standard infrared source components.

eliminates the high-angle, off-axis radiation which is not useful in normal blackbody applications. Eliminating this unused radiation helps control stray radiation and reduces possible orifice heating. As will be evident later, this component design appears to be effective.

The cavity exit orifice in the heater core cap has a measured diameter of 0.203 in. Immediately in front of this orifice is the copper radiation shielding disk containing an 0.10-in.-diam orifice. These two orifices were measured to be approximately 0.062 in. apart. The actual blackbody output aperture is a commercial pinhole which is soldered into a copper mounting disk of design similar to the radiation shielding disk (see Fig. 11). The two copper disks were machined to form the cold cavity mentioned previously. The disks are each 0.125-in. thick, and with the 0.005-in. indium gasket between them, the separation between the radiation shield orifice and the output aperture is 0.255 in.

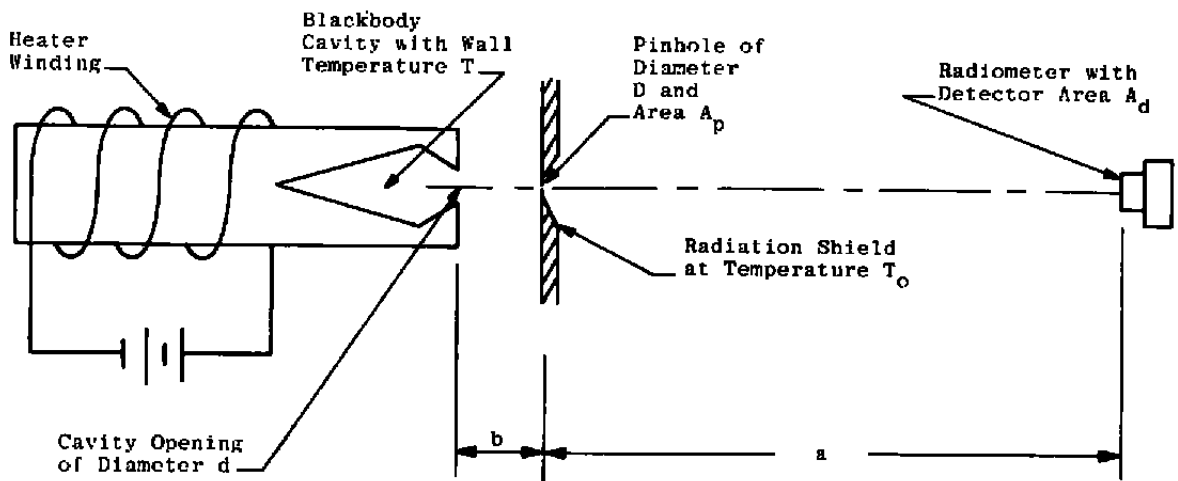
The output aperture itself is a standard, commercial 0.0256-in. Buckbee-Mears pinhole in a thin, 3/8-in.-OD, nickel disk. The aperture diameter was measured at the AEDC on the Benson-Lehner Model 29E® Film Reader (optical comparator) and was determined to be 0.02557 ± 0.00022 in. with a 95-percent confidence interval.

The operation of blackbody infrared sources is best understood by calculating the quantity of radiant power reaching a radiometer through a pinhole located in front of a heated cavity. Assume the experimental arrangement, with defined parameters, as shown in Fig. 12. The solid angle of the radiometer as viewed from the pinhole location is (A_d/a^2) , the detector area divided by the distance squared. When the solid angle is projected backward from the pinhole to the cavity, the area, A_o , of the radiometer "image" at the location of the cavity opening is defined by the equation

$$A_o = b^2 \left(\frac{A_d}{a^2} \right) \tag{1}$$

Therefore, the radiometer is "looking" at an area of the blackbody cavity opening equal to A_o . However, energy flow from the cavity passes through each point in A_o and radiates hemispherically. Very little of the energy emanating from A_o actually reaches the radiometer area. Only those rays that pass through both A_o and the pinhole strike the radiometer. Therefore, the measurement solid angle, Ω_M , is that subtended by the pinhole. It is simply the area, A_p , of the pinhole divided by the square of the distance from the cavity opening to the pinhole

$$\Omega_M = \frac{A_p}{b^2} \tag{2}$$



Conditions.

- (1) $T^4 \gg (T_o)^4$
- (2) $a \geq 10b$

Figure 12. Schematic for analysis of blackbody radiant output.

It is now possible to calculate the amount of power reaching the radiometer. From the Stefan-Boltzmann law, the normal radiant intensity from a blackbody cavity at temperature, T , is $(\sigma T^4/\pi)$ in units of power per unit of cavity output area and solid angle (Ref. 6). The power reaching the radiometer is the product of the measurement solid angle, the effective blackbody area, and the Stefan-Boltzmann equation

$$P = \Omega_M A_o \left(\frac{\sigma T^4}{\pi} \right) \quad (3)$$

From Eqs. (1) and (2):

$$P = b^2 \left(\frac{A_p}{b^2} \right) \left(\frac{A_d}{a^2} \right) \left(\frac{\sigma T^4}{\pi} \right) \quad (4)$$

$$P = \left(\frac{A_p A_d}{a^2} \right) \left(\frac{\sigma T^4}{\pi} \right) \quad (5)$$

It is clear from Eq. (5) that the power reaching the radiometer increases linearly with either A_p , A_d , or T^4 , and decreases according to the inverse square law. In addition, P is completely independent of b , the distance from the cavity opening to the pinhole. Of course, this independence is subject to the condition that A_o be completely contained within the cavity opening. In applications of the SIRS, this condition requires that the radiometer be located on the centerline of the source assembly and have an f /number numerically greater than 2.5.

It is interesting to note that Eq. (5) is simply the normal blackbody output intensity, $\sigma A_p T^4/\pi$, multiplied by the detector solid angle, A_d/a^2 .

This expression for power to the radiometer neglects possible diffraction effects produced by the pinhole. Diffraction effects cause a reduction of energy on the radiometer. The magnitude of diffraction losses for a small area radiometer located on the centerline, as shown in Fig. 12, has been evaluated by Fussell (Ref. 7) to be

$$E'_{\min} = (2.1296 \text{ bd}) \left[\pi^2 DT (d^2 - D^2) \right]^{-1} \quad (6)$$

where the parameters are as defined in Fig. 12, and E'_{\min} is the fractional reduction of total energy on the radiometer. Since E'_{\min} is not a function of the source-to-detector distance, it is

actually a correction to the calculated, normal output intensity, $\sigma A_p T^4/\pi$. For the mechanical dimensions of the SIRS, Eq. (6) can be reduced to

$$E'_{\min} = \frac{9.064}{T} \quad (7)$$

According to Eq. (7), the diffraction loss at 275°K would be 3.296 percent of the output intensity calculated from $\sigma A_p T^4/\pi$. The diffraction losses decrease as the temperature increases. Equation (7) will be employed in Section 4.0, during the bolometer calibration phase.

3.2 CAVITY TEMPERATURE MEASUREMENT AND CONTROL SYSTEM

The temperature measurement and control system for the blackbody cavity is shown in block diagram form in Fig. 13. The blackbody heater is the 12-ohm winding, and the cavity-temperature sensors are the two thermistors. All control circuitry except the Artronix controller is mounted on the AEDC-VKF Standard Infrared Source Control shown in Fig. 14.

The thermistors are Victory Engineering Corporation Type 41A2, which have room-temperature resistances on the order of 10^4 ohms. They exhibit negative temperature coefficients of approximately 4.4 percent per °K. As indicated in Fig. 13, a constant current of $5 \mu\text{A}$ is independently supplied to each thermistor. These bias currents are monitored by measuring the voltage drops (100.00 mV) across precision, 20-k Ω current sampling resistors. With the display selector, either of these voltages may be read on the digital panel meter (DPM). In a similar fashion, the voltage drop across either thermistor may be displayed on the DPM. This voltage drop is the indication of core temperature, and it ranges from about 170 mV at 275°K to about 3 mV at 375°K. The DPM has a full-scale sensitivity of 199.99 mV.

The voltage drop across either thermistor may be used as the temperature control signal, depending on the position of the Control Thermistor Selector. The control signal is amplified by a factor of ten in the Analog Devices Type 275L[®] isolation amplifier and then fed to the Artronix temperature controller. The controller electronically compares the signal to an internal, preset reference signal and automatically raises or lowers the heater supply voltage as required to equalize the control and reference signals. The heater supply circuit from the Artronix controller is fed back through the source control panel so heater current can be monitored and fused. In addition, a 50-ohm current-limiting rheostat is installed in the circuit to provide a load during initial warmup. This is necessary because the resistance of the platinum heater winding is nearly zero when the blackbody has cold-soaked to 20°K. After the cavity is heated to 275°K or above, the rheostat resistance should be adjusted to zero for best control action from the Artronix controller.

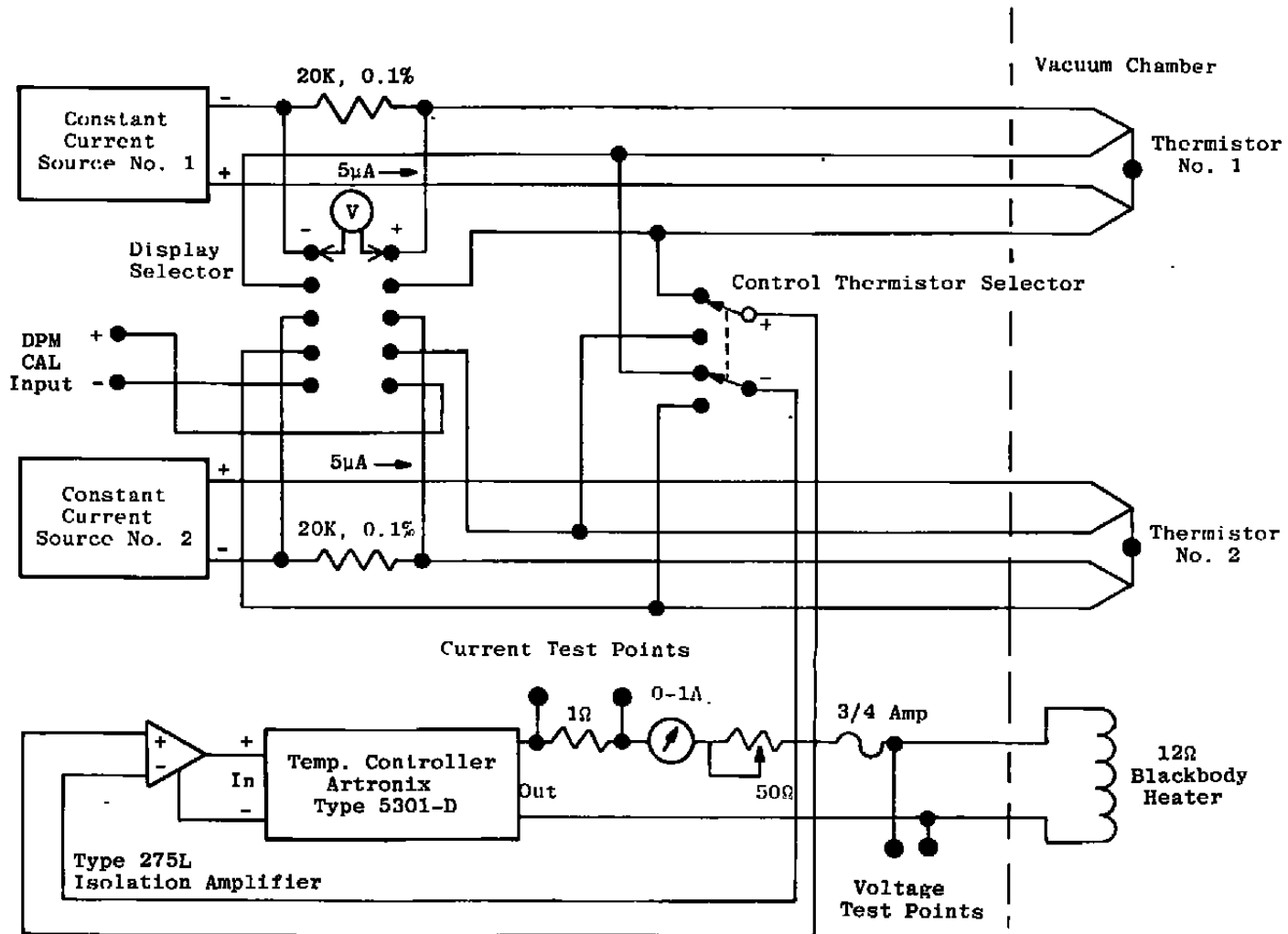


Figure 13. Block diagram of AEDC-VKF standard infrared source control system.

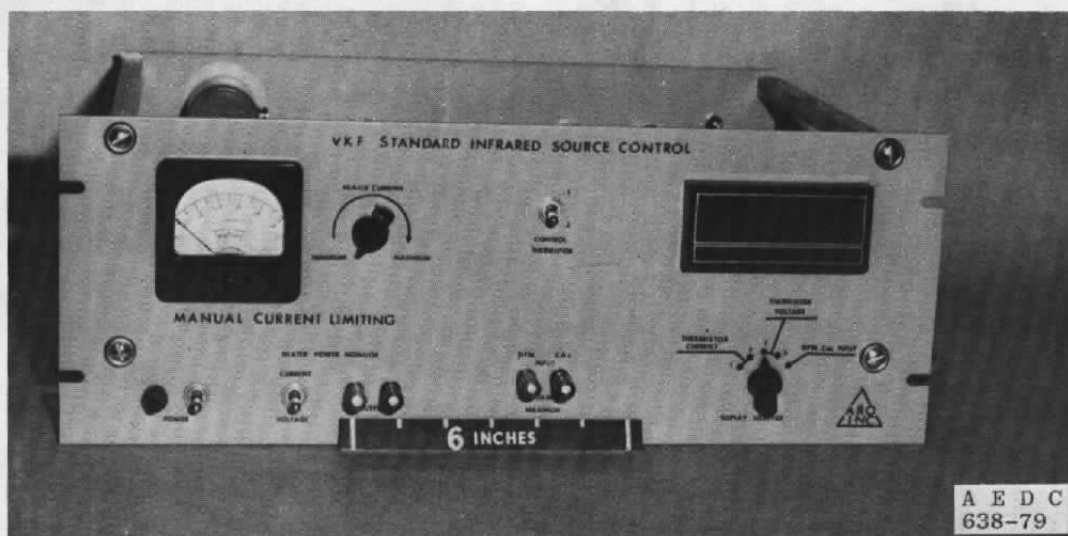


Figure 14. Photograph of AEDC-VKF, standard infrared source control panel.

The primary operating range of the SIRS is from 275 to 375°K. This limitation results from use of thermistors as cavity temperature sensors. When cooled below 275°K, the thermistor resistances increase sharply toward infinity. Above 375°K, these resistances become low and change slowly with temperature. These limitations are tolerated because the thermistors have very high resolution in the primary range of interest from 275 to 375°K and provide the means for precisely repeating cavity temperature settings. To illustrate, the voltage drop across either thermistor is approximately 50 mV at room temperature and it changes at the rate of 2.2 mV per degree K. The least significant digit on the DPM is 0.01 mV, which yields a resolution of 4.5×10^{-3} °K. This resolution is almost three orders of magnitude smaller than the uncertainty of the NBS calibration of the source radiance temperature (see Appendix). Consequently, errors caused by uncertainties in source temperature settings are negligible and can be ignored.

Before the thermistors were installed in the SIRS heater core, they were first placed in a temperature calibration chamber and thermally cycled between LN₂ temperature and 150°C four times. After temperature cycling, the thermistor voltages were calibrated versus temperature with 5 μA of thermistor bias current. The calibration results are presented in Table 1.

In addition to high thermometric resolution, thermistors have another useful operational feature in that the natural log of the voltage drop is very nearly a linear function of inverse absolute temperature. Therefore, it is very practical to use a least-squares, polynomial curve

Table 1. Thermistor Calibration Data

| Temperature, °K | Thermistor No. 1 | | Thermistor No. 2 | |
|--------------------|----------------------|-------------------------|----------------------|-------------------------|
| | Resistance (Ohms) | mV Drop at 5 μ A | Resistance (Ohms) | mV Drop at 5 μ A |
| 268.1 | 41,500 | 207.50 | 47,970 | 239.85 |
| 273.5 | 31,300 | 156.50 | 36,480 | 182.40 |
| 278.1 | 24,830 | 124.15 | 28,900 | 144.50 |
| 283.3 | 19,270 | 96.35 | 22,500 | 112.50 |
| 288.2 | 15,390 | 76.95 | 17,920 | 89.60 |
| 293.2 | 12,200 | 61.00 | 14,250 | 71.25 |
| 298.2 | 9,780 | 48.90 | 11,420 | 57.10 |
| 303.2 | 7,870 | 39.35 | 9,200 | 46.00 |
| 311.8 | 5,600 | 28.00 | 6,490 | 32.45 |
| 323.3 | 3,530 | 17.65 | 4,120 | 20.60 |
| 348.4 | 1,420 | 7.10 | 1,690 | 8.45 |
| 403.7 | 293 | 1.46 | 342 | 1.71 |

fit to represent a thermistor calibration. The data in Table I were used to calculate curve fits for the SIRS thermistors. The resulting operating equations for thermistors 1 and 2, respectively, are

$$\begin{aligned} \frac{1000}{T} = & 2.37427 + 2.79430 \times 10^{-1} (\ln e_T) & (8) \\ & - 2.37121 \times 10^{-2} (\ln e_T)^2 \\ & + 6.14412 \times 10^{-3} (\ln e_T)^3 \\ & - 4.86219 \times 10^{-4} (\ln e_T)^4 \end{aligned}$$

$$\begin{aligned} \frac{1000}{T} = & 2.34306 + 2.51712 \times 10^{-1} (\ln e_T) & (9) \\ & - 4.94094 \times 10^{-3} (\ln e_T)^2 \\ & + 1.54903 \times 10^{-3} (\ln e_T)^3 \\ & - 1.10585 \times 10^{-4} (\ln e_T)^4 \end{aligned}$$

The SIRS cavity temperature is determined simply by reading the two e_T values on the DPM, substituting the values into Eqs. (8) and (9) in the proper order, and calculating solutions.

No formal attempt was made to establish uncertainties in temperatures calculated from Eqs. (8) and (9), because there was no real necessity to do so. The temperatures calculated from Eqs. (8) and (9) are merely indicated core temperatures which provide parameters to base the NBS calibration upon. That is, the radiometric calibration performed by the NBS defines the actual blackbody radiance temperature of the SIRS in terms of the indicated core temperature calculated from Eq. (8) [see Eq. (1) in the Appendix].

3.3 SUMMARY OF THE NBS CALIBRATION RESULTS

The NBS calibration report for the SIRS is presented in the Appendix and is mostly self-explanatory. The center column of Table 1 in the Appendix lists indicated core temperatures, as calculated from Eq. (8). The right column shows the corresponding blackbody radiance temperatures, as determined by the NBS calibration and represented by Eq. (1) in the Appendix. The differences between these temperature values are small, and range from 0.53°K at 270°K to 0.12°K at 391°K. The temperatures calculated from Eq. (1) in the Appendix are the correct values to use in the Stefan-Boltzmann equation when calculating the radiant intensity of the SIRS.

The NBS report also presents information on the uncertainties of the blackbody radiance temperatures as defined by Eq. (1) in the Appendix. Part of this information is shown in Fig. (1) in the Appendix which lists curve fit uncertainties in the blackbody radiance temperatures. It is a simple exercise to differentiate the Stefan-Boltzmann equation and show that the uncertainty in emissive power from a blackbody is four times the uncertainty in blackbody cavity temperature. Therefore, the curve fit uncertainties listed in Fig. 1 of the Appendix contribute up to 1 percent of uncertainty in emissive power. Another 4 percent of uncertainty comes from the factors defined in Table 4 of the Appendix. Combining these factors (in the most pessimistic way) gives a total uncertainty of ± 5 percent in the output intensity of the SIRS.

The NBS calibration report did not supply statistical data on the uncertainties listed in Table 4 of the Appendix. Therefore, it will be assumed that the ± 5 -percent total uncertainty above can be used with a 100-percent confidence interval and it will be taken as the bias error during the calibration of the Molecron bolometer with the SIRS (see Section 4.0).

4.0 BOLOMETER CALIBRATION PROCEDURE AND RESULTS

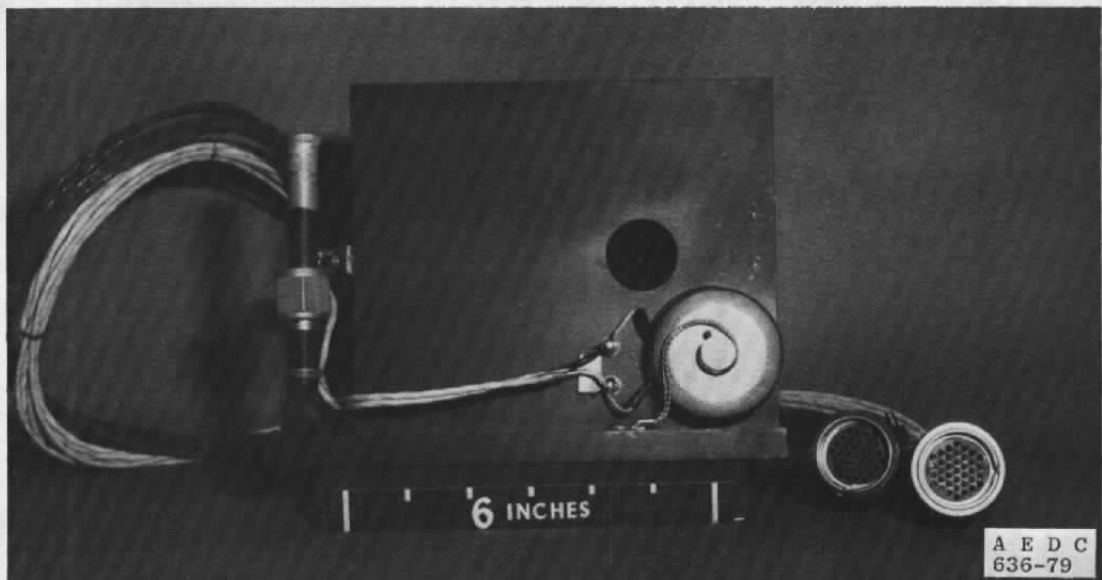
After the SIRS was calibrated at the NBS and returned to the AEDC, preparations were made to use it in the calibration of the Molecron bolometer. The SIRS was mounted on an actively cooled baseplate, along with a chopper and shutter. The chopper and shutter are

required for making unambiguous bolometric measurements. Figures 15a and b show front and rear views of the assembly. The shutter drive is a 45-deg rotary solenoid which is mounted so that the shutter is normally open. The shutter blade (not visible in the photographs) moves between the chopper blade and the output aperture of the SIRS. The chopper wheel (Fig. 15b) runs between a light-emitting diode (LED) and a photo-transistor which puts out a chopper reference signal. This reference signal is required by the lock-in voltmeter that measures the bolometer output signal.

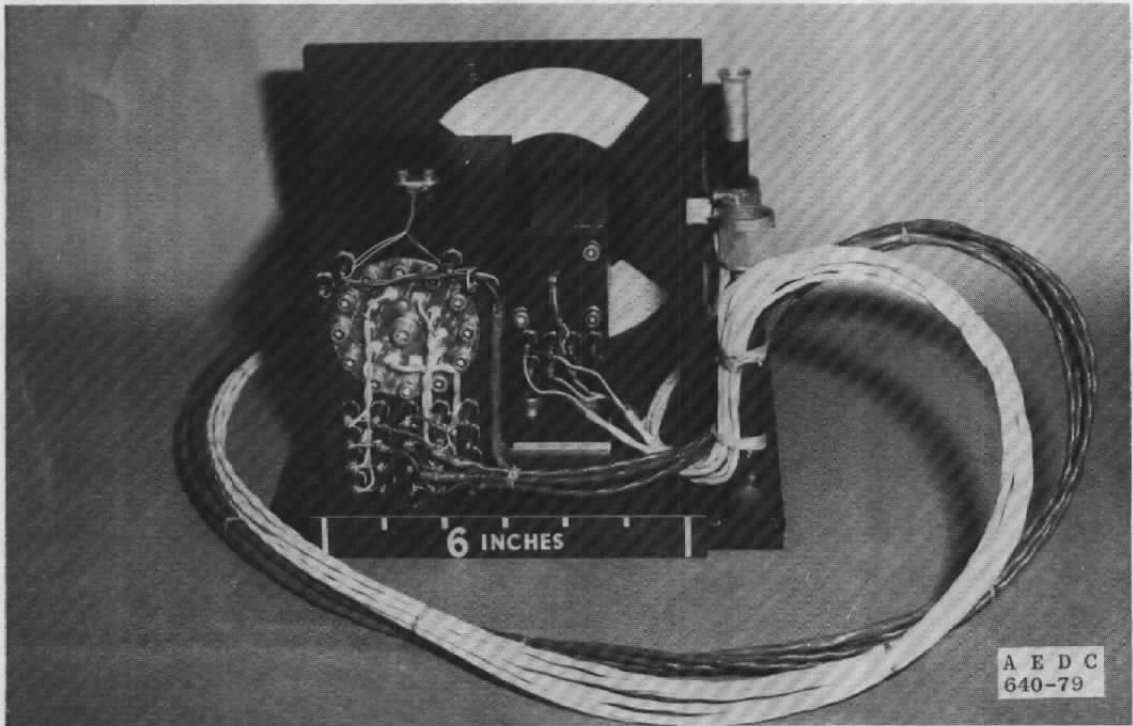
Figure 16 shows the assembly mounted in front of the bolometer in the test chamber. The only part of the bolometer visible in Fig. 16 is the rear cap identified in Fig. 9a. The coiled leads coming off the bottom of the LHe dewar (Fig. 16) are the bolometer circuit leads.

The LHe dewar holds 5 liters of liquid helium, which is pumped by a 13-cfm vacuum pump. The helium gas is pumped through a vacuum regulator valve which stabilizes the helium vapor pressure and, consequently, the bolometer operating temperature and responsivity. The helium vapor pressure is maintained constant at 0.09 psi, and at this pressure a charge of helium will last approximately 24 hours.

The helium vapor pressure is only one of several factors that affect the bolometer responsivity (Ref. 4). Therefore, the only practical way to use the bolometer in radiometric calibrations is to adopt a standard set of auxiliary equipment and operational conditions for the bolometer. The set finally adopted is reviewed in the following discussion.



a. Front view of performance testing assembly
Figure 15. Performance testing assembly.



b. Rear view of performance testing assembly
Figure 15. Concluded.

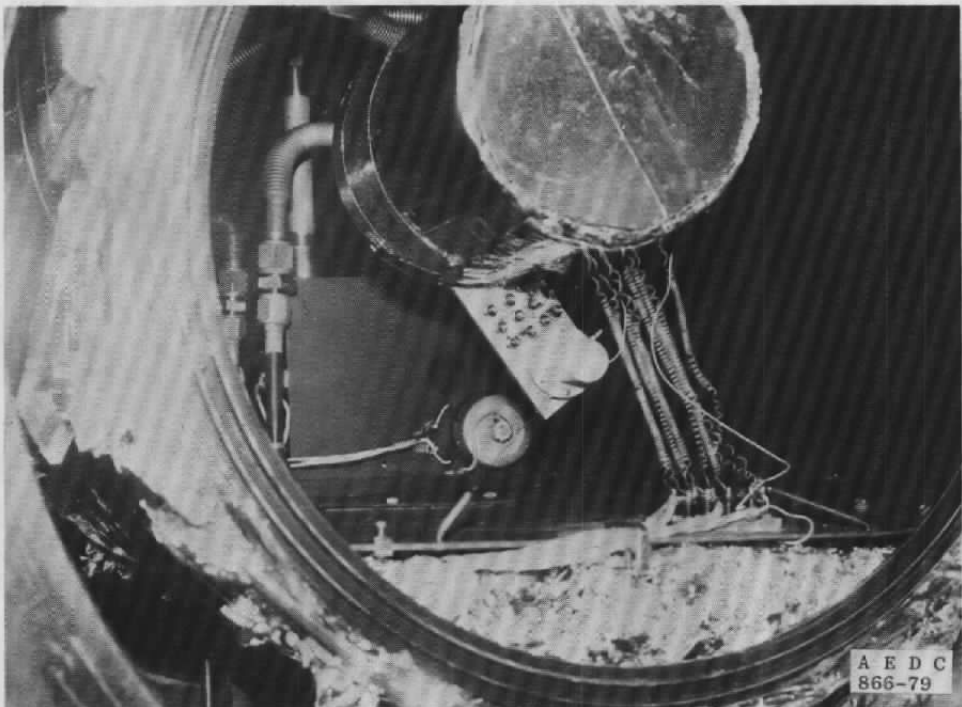


Figure 16. Test chamber installation.

Figure 17 shows the instrumentation system, which includes the bolometer, a M104 MOSFET emitter follower, a constant current source to supply bolometer bias current, a unity gain preamplifier, and a Princeton Applied Research Model HR-8 lock-in amplifier to measure the output signal. The sync signal for the lock-in amplifier is the chopper reference signal from the LED-phototransistor pair mentioned previously. All data were taken at 3 Hz chopping frequency. The bolometer bias current was kept at $0.25 \mu\text{A}$, which is the value at which the bolometer responsivity is maximum (Ref. 4). The distance from the bolometer element to the output aperture of the SIRS was 11.52 in. at room temperature. Future source calibrations must be run at this same distance. It is not known exactly how this distance changes at cryogenic temperatures, but it is assumed that the changes will repeat during future source calibrations.

The calibration of the bolometer was actually a calibration of the entire operating system as described above. That is, an end-to-end system calibration was performed. The end product was a calibration of the HR-8 readings of output signal (volts) as a function of normal output intensity (watts/sr) of the SIRS. The HR-8 reads the rms voltage of the fundamental component of the square wave from the bolometer system, and the data are reported in these units. Although the infrared radiation is chopped with a 50-percent duty cycle chopper, the intensity will be reported in units of peak-to-peak watts. That is, the reported intensity will be in the same units as unchopped blackbody intensity.

The role of the bolometer heater in the overall calibration process is very important. Experience has shown that the data from the bolometer system described above are affected by drifts in the bolometer system responsivity (i.e., output volts per unit input power). However, the ratio of the bolometer responsivities to heater power and to radiometric power seems to be very stable (Ref. 4). This fact is fully exploited by adopting a standard heater voltage to use in monitoring the long-term drifts in bolometer system responsivity. The heater voltage used is the 5-mV (rms of fundamental component) "calibrate" signal available on the front of the HR-8. The long-term variations of this signal do not exceed ± 0.1 percent of magnitude. The bolometer system's response to this 5 mV of heater signal is 40 mV of output signal, with long-term variations of about ± 10 percent. Therefore, 40 mV is taken as the average response, and the mechanics of using the bolometer heater to help correct for drifts in bolometer system responsivity are as follows. Immediately after each radiometric data point is taken, the shutter in front of the SIRS is closed and the 5-mV calibrator signal is applied to the bolometer heater. The resulting bolometer system response is recorded. This signal is then divided into 40 mV, and the calculated correction factor is multiplied by the radiometric data point. This procedure is very effective in correcting for drifts in bolometer system responsivity. Under the assumption that the source-to-bolometer

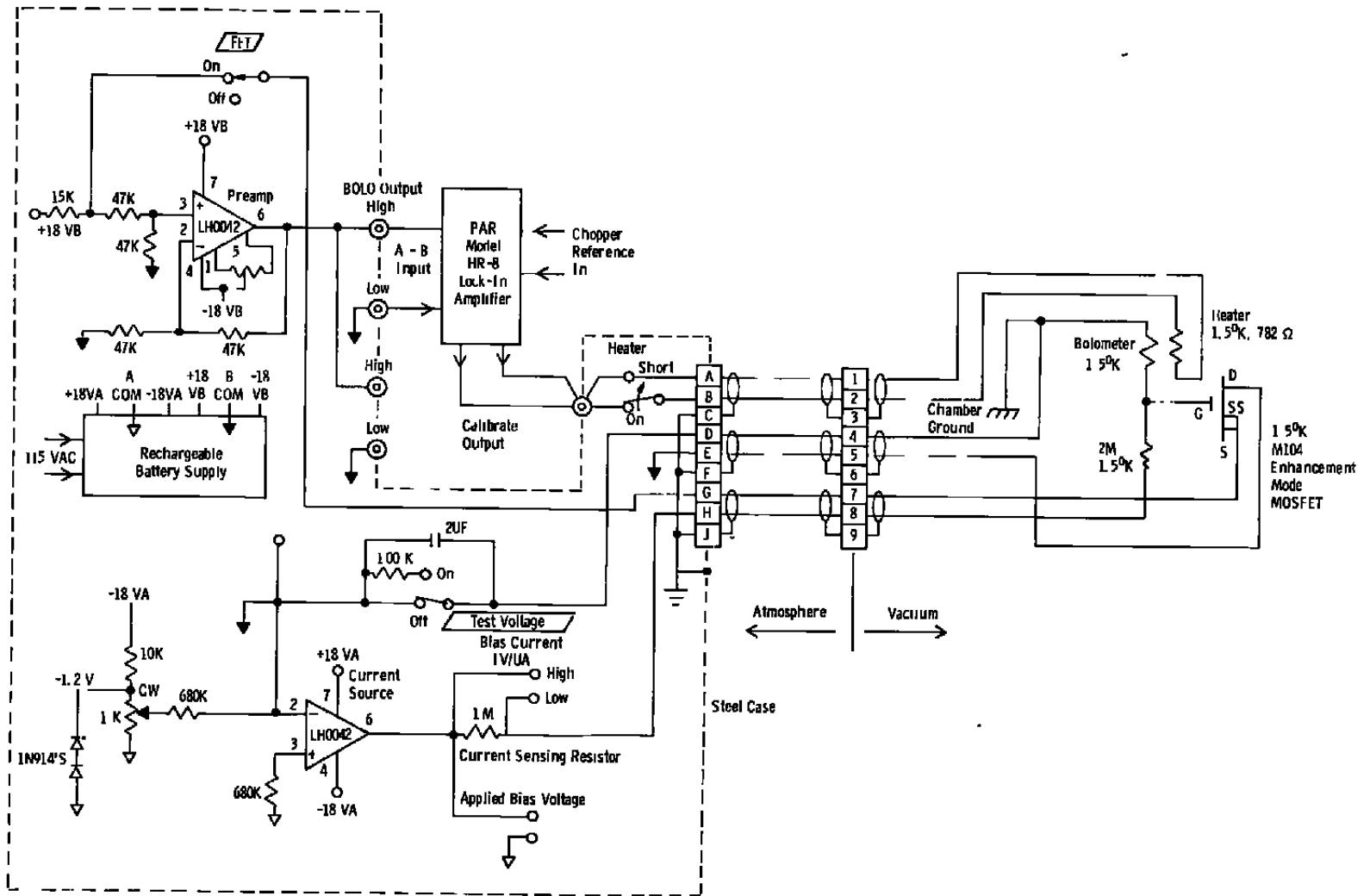


Figure 17. Bolometer instrumentation system schematic.

distance is constant, the procedure corrects for virtually all factors affecting the radiometric data. The only known exception is possible stray radiation originating from chopper heating or other sources.

Three sets of bolometer calibration data were taken, using the SIRS as the standard source. The data were collected and processed as outlined in the discussions above. A set of data consists of data points every 25°K, starting at the SIRS cavity temperature of 275°K and ending at 375°K. A complete set of data was taken each day for three successive days. The results are presented in Table 2. The data are grouped in rows, according to nominal cavity temperature, for ease in comparing day-to-day readings. Actually, each experimental data point presented in Table 2 is the average of four readings taken within the period of about five minutes. This procedure was followed to eliminate reading errors and to average the random, short-term drifts. Therefore, Table 2 represents a total of 60 data readings, although only 15 averages are listed. The core temperatures shown in columns three and five were calculated from the experimental data in columns two and four, using Eqs. (8) and (9), respectively. As explained previously, the bolometer system response to applying 5 mV (rms of fundamental component) to the bolometer heater was monitored and these data are shown in the last column of Table 2. Each reading in this column was divided into 40 mV and this ratio was multiplied by the corresponding radiometric data point. The resulting corrected radiometric data are listed in column 4 of Table 3. The core temperatures indicated by thermistor circuit one and listed in column 3 of Table 2, were corrected according to the NBS calibration specified by Eq. (1) in the Appendix. The corrected radiance temperatures are listed in column 1 of Table 3. Column 2 of Table 3 is the output intensity calculated from the Stefan-Boltzman equation, $\sigma A_p T^4 / \pi$, where T is the corrected radiance temperatures of column 1. According to the NBS calibration, the total uncertainty in this output intensity is ± 5 percent when calculated with the corrected radiance temperatures and then corrected for diffraction effects.

The final correction for diffraction effects can now be made. The data of column 2, Table 3, is multiplied by the factor $(1 - E'_{min})$ where E'_{min} is calculated for each temperature setting, using Eq. (7). Column 3 lists the final corrected output intensities at each radiance temperature.

Column 4 of Table 3 lists the corrected bolometer system output signals, as discussed earlier. The final bolometer system responsivity calibrations are established by dividing the data points in column 4 by the respective data points in column 3. The final responsivity values are listed in the last column. As expected, the data show that the bolometer system responsivity is independent of radiance temperature. However, all of the data points taken the first day are slightly higher than the corresponding data points taken the second and

third days. This indicates the possibility of a small stray radiation problem and suggests that the chamber should be cooled longer before performing calibrations.

Table 2. Experimental Results of Calibration of the Bolometer System with the SIRS

| Nominal Cavity Temperature, °K | Thermistor No. 1 | | Thermistor No. 2 | | Bolometer System Response HR-8 Indication, mV | |
|--------------------------------|------------------|--------|------------------|--------|---|--------------------|
| | mV | °K | mV | °K | Radiometric Data | Response to Heater |
| 275 | 144.06 | 275.10 | 168.84 | 274.98 | 2.77 | 39.27 |
| | 144.46 | 275.05 | 169.31 | 274.93 | 2.62 | 38.01 |
| | 144.45 | 275.05 | 169.02 | 274.96 | 2.65 | 38.45 |
| 300 | 44.50 | 300.45 | 52.25 | 300.27 | 3.95 | 39.29 |
| | 44.55 | 300.43 | 52.35 | 300.23 | 3.79 | 38.61 |
| | 44.57 | 300.42 | 52.23 | 300.28 | 3.80 | 38.89 |
| 325 | 16.59 | 324.89 | 19.52 | 324.74 | 5.55 | 39.36 |
| | 16.79 | 324.58 | 19.76 | 324.41 | 5.26 | 38.62 |
| | 16.80 | 324.56 | 19.78 | 324.39 | 5.30 | 39.04 |
| 350 | 6.84 | 349.54 | 8.07 | 349.76 | 7.57 | 39.34 |
| | 6.84 | 349.54 | 8.08 | 349.72 | 7.12 | 39.51 |
| | 6.84 | 349.54 | 8.07 | 349.76 | 7.18 | 39.07 |
| 375 | 3.06 | 375.24 | 3.64 | 375.51 | 10.07 | 39.36 |
| | 3.07 | 375.13 | 3.64 | 375.51 | 9.57 | 38.62 |
| | 3.06 | 375.24 | 3.63 | 375.60 | 9.58 | 38.98 |

The average (\bar{r}) of the 15 responsivity values (r_i) is 85.43 volts/(watt/sr); and the precision index (i.e., the best estimate of standard deviation) is calculated from the expression

$$s = \sqrt{\frac{\sum_{i=1}^n (r_i - \bar{r})^2}{(n - 1)}} \tag{10}$$

The index n equals 15, the number of measured responsivity values, and the calculated value of s is 1.733 volts/(watt/sr).

The objective at this point is to statistically process the measured responsivity values in order to determine the true bolometer system responsivity value, \bar{R} . Assuming that the r_i samples come from a normal (Gaussian) distribution, then

$$\bar{R} = \left(\bar{r} \pm \frac{t_{\alpha/2}^s}{\sqrt{n}} \right) \pm \bar{r}B \quad (11)$$

where $t_{\alpha/2}$ is (Ref. 8) the two-tailed Student's t for the confidence interval $(1 - \alpha)$, and B is the bias error (0.05) from the NBS calibration data (see Section 3.3). For a 99-percent confidence interval, $t_{0.005} = 2.977$. Substituting the experimental values into Eq. (11) gives

$$\bar{R} = \left(85.43 \pm \frac{2.977 \times 1.733}{\sqrt{15}} \right) \pm (85.43 \times 0.05) \quad (12)$$

or

$$\bar{R} = (85.43 \pm 1.332) \pm 4.272 \quad (13)$$

Therefore

$$\bar{R} = 85.43 \pm 5.60 \text{ [volts/(watt./sr)]} \quad (14)$$

Table 3. Summary of Bolometer System Responsivity Calibrations

| Blackbody Radiance Temp., °K | SIRS Output Intensity x 10 ⁵ , watts/sr | Diffraction Corrected Output Intensity x 10 ⁵ , watts/sr | Sensitivity Corrected Bolometer System Reponse, mV | Bolometer System Responsivity, volt/(watts/sr) |
|------------------------------|--|---|--|--|
| 274.59 | 3.399 | 3.287 | 2.821 | 85.82 |
| 274.54 | 3.396 | 3.284 | 2.757 | 83.95 |
| 274.54 | 3.396 | 3.284 | 2.757 | 83.95 |
| 300.03 | 4.844 | 4.698 | 4.021 | 85.60 |
| 300.01 | 4.843 | 4.697 | 3.926 | 83.59 |
| 300.00 | 4.860 | 4.713 | 3.908 | 82.92 |
| 324.55 | 6.633 | 6.448 | 5.640 | 87.47 |
| 324.23 | 6.607 | 6.422 | 5.448 | 84.83 |
| 324.22 | 6.606 | 6.421 | 5.430 | 84.57 |
| 349.28 | 8.897 | 8.666 | 7.697 | 88.82 |
| 349.28 | 8.897 | 8.666 | 7.395 | 85.33 |
| 349.28 | 8.897 | 8.666 | 7.351 | 84.83 |
| 375.07 | 11.831 | 11.545 | 10.234 | 88.64 |
| 374.96 | 11.817 | 11.531 | 9.912 | 85.96 |
| 375.07 | 11.831 | 11.545 | 9.831 | 85.15 |

This is a total uncertainty of ± 6.56 percent, with a confidence interval of 99 percent.

The result in Eq. (14) is the final product of this calibration effort. It is the Molelectron bolometer responsivity for the standard operating equipment and conditions defined earlier. It is important to emphasize that these standard conditions include the separation (11.52 in.) of the blackbody aperture and the bolometer element. In future calibrations where the result of Eq. (14) is used, it is imperative to install the blackbody at the 11.52-in. separation. The error analysis of the future calibration data must include a term representing the uncertainty of re-establishing the 11.52-in. separation.

5.0 SUMMARY

A working-standard low-temperature blackbody has been developed and used to transfer a radiometric calibration from the NBS facility to the AEDC. The source was used to establish a radiometric calibration of the Molelectron bolometer responsivity. The bolometer's responsivity to point source intensity is 85.43 [volts/(watt/sr)] when the separation from point source to bolometer element was set at 11.52 in. (room temperature setting). The total uncertainty in the responsivity determination is ± 6.56 percent of magnitude, with a statistical confidence interval of 99 percent. The bolometer is now being used to calibrate various operational low-temperature blackbody sources, including the reference blackbody in the 7V radiation monitor telescope. These additional calibrations are being performed as a part of the SIRE sensor test preparations.

REFERENCES

1. Arnold, F. and Nelms, F. W. "AEDC Long Wavelength Infrared Test Facilities." *Optical Engineering*, Vol. 15, No. 6, November-December 1976, pp. 549-553.
2. Yokley, C. R. "A Radiometric Calibration Facility for Low Temperature Blackbodies." Final Report on Order No. T-9550C, National Bureau of Standards, Washington, DC, November 1976.
3. Kunz, L. W. "An Improved Silicon Bolometer with Self-Calibrating Capability." *Proceedings of the Society of Photo-Optical Instrumentation Engineers*, Vol. 67, 1975, pp. 37-40.
4. Belew, P. W. and Sherrell, F. G. "Evaluation of a Self-Calibrating Silicon Bolometer." AEDC-TR-78-74 (ADA068083), April 1979.

5. Wolfe, W. L. (Editor). *Handbook of Military Infrared Technology*, Library of Congress Catalog No. 65-62266, US Government Printing Office, Washington, DC, 1965.
6. Sparrow, E. M. and Cess, R. D. *Radiation Heat Transfer*. Brooks/Cole Publishing Co., Belmont, CA, 1970 (Revised Edition).
7. Fussell, W. B. "Tables of Diffraction Losses." NBS Technical Note, June 1974.
8. Miller, I. and Freund, J. E. *Probability and Statistics for Engineers*. Prentice-Hall, Inc., Englewood Cliffs, NJ, 1977 (Second Edition).

APPENDIX

U.S. DEPARTMENT OF COMMERCE
NATIONAL BUREAU OF STANDARDS
WASHINGTON, D.C. 20234

REPORT OF CALIBRATION

SPECIAL TEST
Radiance Temperature Calibration
of a
Working Standard Blackbody
for
USAF/AEDC
Arnold Air Force Station, Tennessee

(Procurement Doc. No. 9A-6676-B)

1. Material Submitted

- A. One VKF Working Standard Blackbody with limiting aperture (.02557 inches diameter).
Specified low and high temperature limits of operation are 275 kelvins and 400 kelvins, respectively.
- B. The following apparatus for setting and controlling the temperature:
 - (1) One Airtronix combination power supply and temperature regulator.
 - (2) One instruction set which explains the operation of the VKF controller.
 - (3) Controller power supply cable. Interconnecting cables for the control and monitor resistance thermometers and thermistors were included.
 - (4) Temperature display system and connecting cables.

2. Purpose of the Test

To determine the radiance temperature of the blackbody in the 275 kelvins to 375 kelvins temperature range when the source is operated in a 20 kelvins environmental temperature.

NBS Test No. 534/221273
June 26, 1980

Page 1 of 5

REPORT OF CALIBRATION
Special Test
USAF/AEDC

3. Method and Conditions of Calibration

The blackbody was calibrated using a cryogenic, absolute radiometer which is described in the accompanying report "A Radiometric Calibration Facility for Low Temperature Blackbodies".

The diameter of the blackbody limiting aperture, 0.02557 inches, was obtained from the enclosed instruction set.

With the exception of two cooldowns to 20 kelvins during which the calibration was performed, the blackbody was operated continuously in a 77 kelvins, 10^{-8} Torr environment for about 60 days. The approximate time that the blackbody heat sink was maintained at 20 kelvins was 40 hours. At no time was the cavity temperature permitted to go below 250 kelvins or above 405 kelvins.

The VKF blackbody is an extended source but as used here it is not extended enough to eliminate the need for a diffraction correction. These corrections to the measured flux ranged from 2.5% to 3.5% and the method for obtaining them is described in pages 23 to 28 (equations 1 to 12) in the enclosed Technical Note "Tables of Diffraction Losses".

A massive copper heat sink and calibrated resistance thermometer were included as part of the VKF blackbody system.

An NBS remotely operated shutter was attached to this heat sink in a manner which permitted good thermal coupling between the two devices. Three additional temperature measuring devices (AU/FE thermocouples) were included in the shutter assembly.

In the temperature range 13 to 28 kelvins, the differences between all four measurement devices did not exceed 2 kelvins.

Acceptable data was included in the calibration only when the heat sink temperature did not deviate by more than ± 2 kelvins from a nominal value of 20 kelvins.

4. Source Orientation and Mounting

The general arrangement of the source and radiometer is given in figure A-2.

REPORT OF CALIBRATION
 Special Test
 USAF/AEDC

The VKF blackbody itself was bolted to a copper, actively cooled, liquid helium heat exchanger (supplied by AEDC). An indium gasket was used to facilitate good thermal clamping. The heat exchanger itself was adjusted so that the viewing axis of the VKF blackbody was perpendicular in space to within one degree.

The calibration system provides for translation in two mutually perpendicular directions in the horizontal plane. The blackbody was translated until the radiant signal indicated radiometric center and insured that no cutoff had occurred.

5. Results

The final results of the calibration are presented in Tables 1, 2, 3, and 4, and figure A-1. These results were established by using least square fitting routines and the data collected for 92 radiometric matches throughout the requested temperature calibration range. Two equations were developed and used in conjunction with a third provided by AEDC.

These equations are known as:

$$\text{Eq. 1.} \quad T_R = A_0 + A_1 T_1$$

where T_1 is the thermometric temperature indicated by thermistor circuit 1 and T_R is the calibrated radiance temperature (both are kelvins).

$$A_0 = -1.43799 \quad A_1 = 1.00337$$

$$\text{Eq. 2.} \quad V_2 = B_0 + B_1 V_1 + B_2 V_1^2$$

Here, V_1 is the millivolt output of thermistor circuit one and V_2 is the millivolt output of thermistor circuit 2.

REPORT OF CALIBRATION
 Special Test
 USAF/AEDC

$$B_0 = 2.89559 \times 10^{-2}$$

$$B_1 = 1.17253$$

$$B_2 = -3.58078 \times 10^{-5}$$

Equation 3 is the thermometric calibration provided by AEDC relating T_1 to the natural logarithm of V_1 . It is repeated here for convenience.

$$\text{Eq. 3.} \quad \frac{1000}{T_1} = C_0 + C_1 \ln V_1 + C_2 (\ln V_1)^2 + C_3 (\ln V_1)^3 + C_4 (\ln V_1)^4$$

$$C_0 = 2.37427$$

$$C_1 = 2.7943 \times 10^{-1}$$

$$C_2 = -2.37121 \times 10^{-2}$$

$$C_3 = 6.14412 \times 10^{-3}$$

$$C_4 = -4.86219 \times 10^{-4}$$

Throughout this test, thermistor 2 was used as the control thermistor and thermistor 1, the monitor.

6. Uncertainties

The standard deviation of a predicted value of T_R in the above-mentioned least squares fit varied from 0.57 kelvin at 275 kelvins to 0.95 kelvin at 375 kelvins. (See figure A-1 inset.)

REPORT OF CALIBRATION
Special Test
USAF/AEDC

Table 4 lists various known significant sources of uncertainty relative to the measured radiance. The combination of the various individual uncertainties in quadrature is 1.6% and the sum of their absolute values is 4%. The 4% in radiance corresponds to 3 kelvins at 275 K and 4 kelvins at 375 K.

Principal Investigator

Charles R. Yokley
Charles R. Yokley

For the Director

Chris E. Kuydt /for
Jack L. Tech, Chief
Radiometric Physics Division
Center for Radiation Research

NBS Test No. 534/221273
June 26, 1980

Page 5 of 5

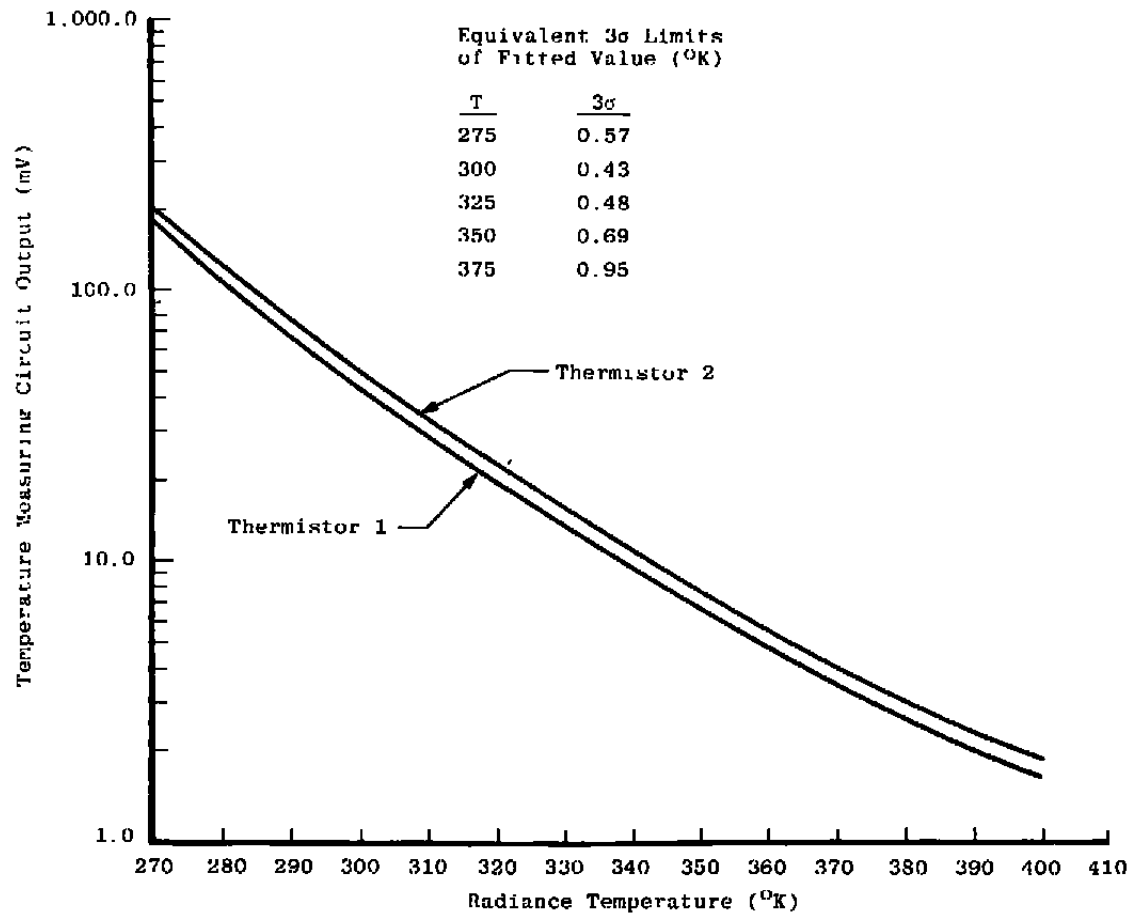
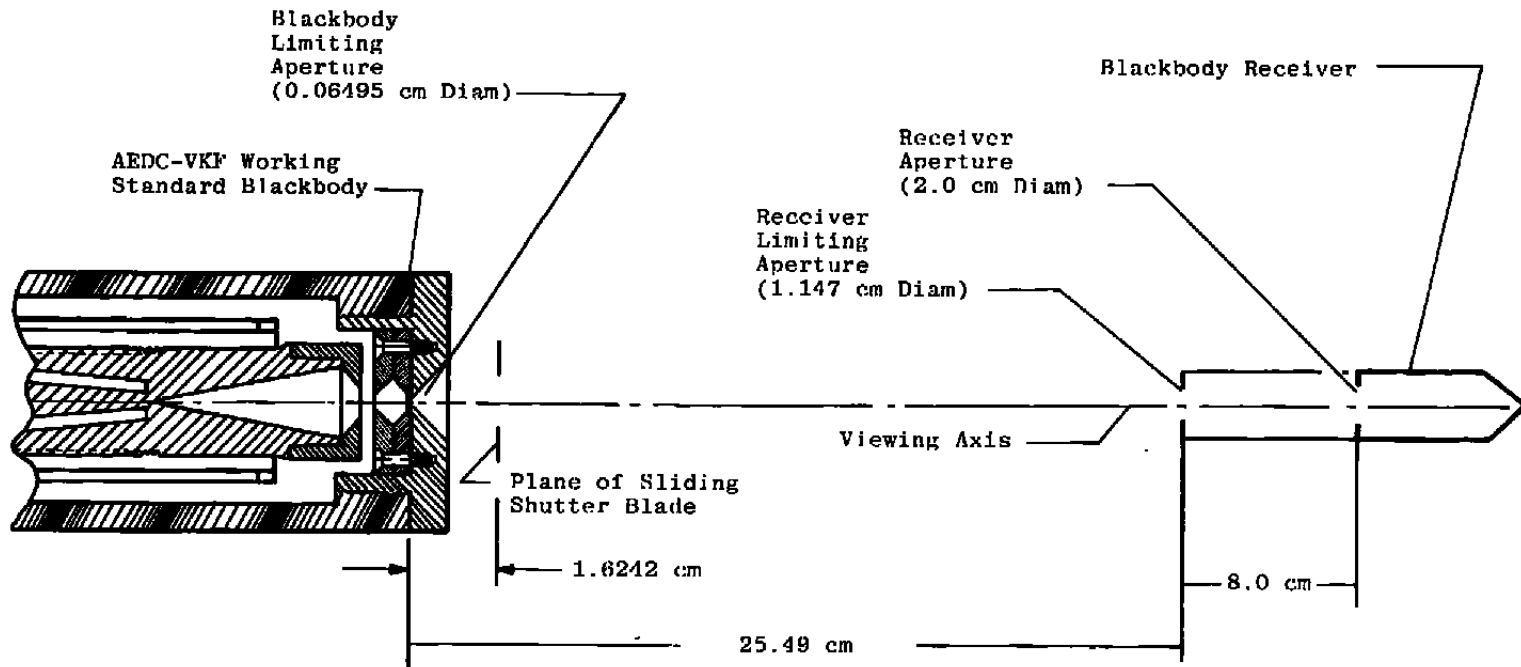


Figure A-1. Calibration of thermistor voltages (at 5 μ A bias current)
vs blackbody radiance temperature.



All Dimensions Referred to 300 Kelvins

Not to Scale

Figure A-2. Schematic diagram of measurement configuration.

Table 1

| THERMISTOR 1 | | | BLACKBODY RADIANCE | | | THERMISTOR 1 | | | BLACKBODY RADIANCE | | |
|--------------|-----------|-----------|--------------------|-----------|-----------|--------------|-----------|-----------|--------------------|-----------|-----------|
| VOLTAGE | TEMP. | TEMP. | VOLTAGE | TEMP. | TEMP. | VOLTAGE | TEMP. | TEMP. | VOLTAGE | TEMP. | TEMP. |
| (MV) | (KELVINS) | (KELVINS) | (MV) | (KELVINS) | (KELVINS) | (MV) | (KELVINS) | (KELVINS) | (MV) | (KELVINS) | (KELVINS) |
| ----- | ----- | ----- | ----- | ----- | ----- | ----- | ----- | ----- | ----- | ----- | ----- |
| 187.84 | 270.00 | 269.47 | 13.19 | 331.00 | 330.68 | 6.87 | 342.00 | 341.71 | | | |
| 178.13 | 271.00 | 270.48 | 12.71 | 332.00 | 331.68 | 6.56 | 343.00 | 342.72 | | | |
| 169.00 | 272.00 | 271.48 | 12.25 | 333.00 | 332.68 | 6.27 | 344.00 | 343.72 | | | |
| 160.45 | 273.00 | 272.48 | 11.81 | 334.00 | 333.69 | 7.99 | 345.00 | 344.72 | | | |
| 152.38 | 274.00 | 273.49 | 11.38 | 335.00 | 334.69 | 7.72 | 346.00 | 345.73 | | | |
| 144.81 | 275.00 | 274.49 | 10.98 | 336.00 | 335.69 | 7.46 | 347.00 | 346.73 | | | |
| 137.65 | 276.00 | 275.49 | 10.59 | 337.00 | 336.70 | 7.21 | 348.00 | 347.73 | | | |
| 130.93 | 277.00 | 276.50 | 10.22 | 338.00 | 337.70 | 6.97 | 349.00 | 348.74 | | | |
| 124.57 | 278.00 | 277.50 | 9.86 | 339.00 | 338.70 | 6.73 | 350.00 | 349.74 | | | |
| 118.59 | 279.00 | 278.50 | 9.51 | 340.00 | 339.71 | 6.51 | 351.00 | 350.74 | | | |
| 112.92 | 282.00 | 279.51 | | | | | | | | | |
| 107.57 | 281.00 | 280.51 | | | | | | | | | |
| 102.49 | 282.00 | 281.51 | | | | | | | | | |
| 97.72 | 283.00 | 282.52 | | | | | | | | | |
| 93.19 | 284.00 | 283.52 | | | | | | | | | |
| 88.90 | 285.00 | 284.52 | | | | | | | | | |
| 84.82 | 286.00 | 285.53 | | | | | | | | | |
| 80.98 | 287.00 | 286.53 | | | | | | | | | |
| 77.31 | 288.00 | 287.53 | | | | | | | | | |
| 73.85 | 289.00 | 288.54 | | | | | | | | | |
| 70.56 | 290.00 | 289.54 | | | | | | | | | |
| | | | | | | | | | | | |
| 67.43 | 291.00 | 290.54 | 6.30 | 352.00 | 351.75 | 6.09 | 353.00 | 352.75 | | | |
| 64.45 | 292.00 | 291.55 | 5.89 | 354.00 | 353.76 | 5.78 | 355.00 | 354.76 | | | |
| 61.64 | 293.00 | 292.55 | 5.52 | 356.00 | 355.76 | 5.34 | 357.00 | 356.77 | | | |
| 58.95 | 294.00 | 293.55 | 5.24 | 358.00 | 357.77 | 5.18 | 358.00 | 357.77 | | | |
| 56.40 | 295.00 | 294.56 | 5.01 | 359.00 | 358.77 | 4.85 | 360.00 | 359.78 | | | |
| 53.98 | 296.00 | 295.56 | 4.78 | 361.00 | 360.78 | | | | | | |
| 51.67 | 297.00 | 296.56 | | | | | | | | | |
| 49.47 | 298.00 | 297.57 | | | | | | | | | |
| 47.37 | 299.00 | 298.57 | | | | | | | | | |
| 45.37 | 300.00 | 299.57 | | | | | | | | | |
| | | | | | | | | | | | |
| 43.47 | 301.00 | 300.58 | 4.56 | 362.00 | 361.78 | 4.42 | 363.00 | 362.79 | | | |
| 41.66 | 302.00 | 301.58 | 4.22 | 364.00 | 363.79 | 4.15 | 365.00 | 364.79 | | | |
| 39.93 | 303.00 | 302.58 | 4.03 | 366.00 | 365.80 | 3.90 | 367.00 | 366.80 | | | |
| 38.28 | 304.00 | 303.59 | 3.90 | 367.00 | 366.80 | 3.79 | 368.00 | 367.80 | | | |
| 36.71 | 305.00 | 304.59 | 3.68 | 369.00 | 368.81 | 3.57 | 370.00 | 369.81 | | | |
| 35.21 | 306.00 | 305.59 | 3.46 | 371.00 | 370.81 | | | | | | |
| 33.78 | 307.00 | 306.60 | | | | | | | | | |
| 32.41 | 308.00 | 307.60 | | | | | | | | | |
| 31.10 | 309.00 | 308.60 | | | | | | | | | |
| 29.85 | 310.00 | 309.61 | | | | | | | | | |
| | | | | | | | | | | | |
| 28.66 | 311.00 | 310.61 | 3.36 | 372.00 | 371.82 | 3.26 | 373.00 | 372.82 | | | |
| 27.52 | 312.00 | 311.61 | 3.17 | 374.00 | 373.82 | 3.08 | 375.00 | 374.83 | | | |
| 26.43 | 313.00 | 312.62 | 2.99 | 376.00 | 375.83 | 2.91 | 377.00 | 376.83 | | | |
| 25.39 | 314.00 | 313.62 | 2.83 | 378.00 | 377.84 | 2.75 | 379.00 | 378.84 | | | |
| 24.40 | 315.00 | 314.62 | 2.67 | 380.00 | 379.84 | 2.60 | 381.00 | 380.85 | | | |
| 23.45 | 316.00 | 315.63 | | | | | | | | | |
| 22.54 | 317.00 | 316.63 | | | | | | | | | |
| 21.66 | 318.00 | 317.63 | | | | | | | | | |
| 20.83 | 319.00 | 318.64 | | | | | | | | | |
| 20.03 | 320.00 | 319.64 | | | | | | | | | |
| | | | | | | | | | | | |
| 19.27 | 321.00 | 320.64 | 2.53 | 382.00 | 381.85 | 2.46 | 383.00 | 382.85 | | | |
| 18.54 | 322.00 | 321.65 | 2.40 | 384.00 | 383.86 | 2.33 | 385.00 | 384.86 | | | |
| 17.83 | 323.00 | 322.65 | 2.27 | 386.00 | 385.86 | 2.21 | 387.00 | 386.87 | | | |
| 17.16 | 324.00 | 323.65 | 2.15 | 388.00 | 387.87 | 2.10 | 389.00 | 388.87 | | | |
| 16.52 | 325.00 | 324.66 | 2.04 | 390.00 | 389.88 | 1.99 | 391.00 | 390.88 | | | |
| 15.91 | 326.00 | 325.66 | | | | | | | | | |
| 15.31 | 327.00 | 326.66 | | | | | | | | | |
| 14.75 | 328.00 | 327.67 | | | | | | | | | |
| 14.20 | 329.00 | 328.67 | | | | | | | | | |
| 13.68 | 330.00 | 329.67 | | | | | | | | | |

NBS Test No. 534/221273
June 26, 1980

Table 2

| THERMISTOR 2 | | | BLACKBODY RADIANCE | | | THERMISTOR 2 | | | BLACKBODY RADIANCE | | |
|--------------|-----------------|-----------------|--------------------|-----------------|-----------------|--------------|-----------------|-----------------|--------------------|-----------------|-----------------|
| VOLTAGE (MV) | TEMP. (KELVINS) | TEMP. (KELVINS) | VOLTAGE (MV) | TEMP. (KELVINS) | TEMP. (KELVINS) | VOLTAGE (MV) | TEMP. (KELVINS) | TEMP. (KELVINS) | VOLTAGE (MV) | TEMP. (KELVINS) | TEMP. (KELVINS) |
| 219.01 | 270.00 | 269.47 | 15.48 | 331.00 | 330.68 | 15.48 | 331.00 | 330.68 | 15.48 | 331.00 | 330.68 |
| 207.76 | 271.00 | 270.48 | 14.92 | 332.00 | 331.68 | 14.92 | 332.00 | 331.68 | 14.92 | 332.00 | 331.68 |
| 197.16 | 272.00 | 271.48 | 14.38 | 333.00 | 332.68 | 14.38 | 333.00 | 332.68 | 14.38 | 333.00 | 332.68 |
| 187.24 | 273.00 | 272.48 | 13.87 | 334.00 | 333.69 | 13.87 | 334.00 | 333.69 | 13.87 | 334.00 | 333.69 |
| 177.87 | 274.00 | 273.49 | 13.37 | 335.00 | 334.69 | 13.37 | 335.00 | 334.69 | 13.37 | 335.00 | 334.69 |
| 169.07 | 275.00 | 274.49 | 12.90 | 336.00 | 335.69 | 12.90 | 336.00 | 335.69 | 12.90 | 336.00 | 335.69 |
| 160.75 | 276.00 | 275.49 | 12.44 | 337.00 | 336.70 | 12.44 | 337.00 | 336.70 | 12.44 | 337.00 | 336.70 |
| 152.94 | 277.00 | 276.50 | 12.01 | 338.00 | 337.70 | 12.01 | 338.00 | 337.70 | 12.01 | 338.00 | 337.70 |
| 145.54 | 278.00 | 277.50 | 11.58 | 339.00 | 338.70 | 11.58 | 339.00 | 338.70 | 11.58 | 339.00 | 338.70 |
| 138.57 | 279.00 | 278.50 | 11.18 | 340.00 | 339.71 | 11.18 | 340.00 | 339.71 | 11.18 | 340.00 | 339.71 |
| 131.96 | 280.00 | 279.51 | 10.79 | 341.00 | 340.71 | 10.79 | 341.00 | 340.71 | 10.79 | 341.00 | 340.71 |
| 125.74 | 281.00 | 280.51 | 10.42 | 342.00 | 341.71 | 10.42 | 342.00 | 341.71 | 10.42 | 342.00 | 341.71 |
| 119.83 | 282.00 | 281.51 | 10.06 | 343.00 | 342.72 | 10.06 | 343.00 | 342.72 | 10.06 | 343.00 | 342.72 |
| 114.27 | 283.00 | 282.52 | 9.72 | 344.00 | 343.72 | 9.72 | 344.00 | 343.72 | 9.72 | 344.00 | 343.72 |
| 108.99 | 284.00 | 283.52 | 9.39 | 345.00 | 344.72 | 9.39 | 345.00 | 344.72 | 9.39 | 345.00 | 344.72 |
| 103.98 | 285.00 | 284.52 | 9.07 | 346.00 | 345.73 | 9.07 | 346.00 | 345.73 | 9.07 | 346.00 | 345.73 |
| 99.23 | 286.00 | 285.53 | 8.77 | 347.00 | 346.73 | 8.77 | 347.00 | 346.73 | 8.77 | 347.00 | 346.73 |
| 94.74 | 287.00 | 286.53 | 8.48 | 348.00 | 347.73 | 8.48 | 348.00 | 347.73 | 8.48 | 348.00 | 347.73 |
| 90.47 | 288.00 | 287.53 | 8.19 | 349.00 | 348.74 | 8.19 | 349.00 | 348.74 | 8.19 | 349.00 | 348.74 |
| 86.43 | 289.00 | 288.54 | 7.92 | 350.00 | 349.74 | 7.92 | 350.00 | 349.74 | 7.92 | 350.00 | 349.74 |
| 82.59 | 290.00 | 289.54 | 7.66 | 351.00 | 350.74 | 7.66 | 351.00 | 350.74 | 7.66 | 351.00 | 350.74 |
| 78.93 | 291.00 | 290.54 | 7.41 | 352.00 | 351.75 | 7.41 | 352.00 | 351.75 | 7.41 | 352.00 | 351.75 |
| 75.45 | 292.00 | 291.55 | 7.17 | 353.00 | 352.75 | 7.17 | 353.00 | 352.75 | 7.17 | 353.00 | 352.75 |
| 72.17 | 293.00 | 292.55 | 6.94 | 354.00 | 353.76 | 6.94 | 354.00 | 353.76 | 6.94 | 354.00 | 353.76 |
| 69.02 | 294.00 | 293.55 | 6.72 | 355.00 | 354.76 | 6.72 | 355.00 | 354.76 | 6.72 | 355.00 | 354.76 |
| 66.05 | 295.00 | 294.56 | 6.50 | 356.00 | 355.76 | 6.50 | 356.00 | 355.76 | 6.50 | 356.00 | 355.76 |
| 63.21 | 296.00 | 295.56 | 6.29 | 357.00 | 356.77 | 6.29 | 357.00 | 356.77 | 6.29 | 357.00 | 356.77 |
| 60.51 | 297.00 | 296.56 | 6.10 | 358.00 | 357.77 | 6.10 | 358.00 | 357.77 | 6.10 | 358.00 | 357.77 |
| 57.94 | 298.00 | 297.57 | 5.90 | 359.00 | 358.77 | 5.90 | 359.00 | 358.77 | 5.90 | 359.00 | 358.77 |
| 55.49 | 299.00 | 298.57 | 5.72 | 360.00 | 359.78 | 5.72 | 360.00 | 359.78 | 5.72 | 360.00 | 359.78 |
| 53.16 | 300.00 | 299.57 | 5.54 | 361.00 | 360.78 | 5.54 | 361.00 | 360.78 | 5.54 | 361.00 | 360.78 |
| 50.93 | 301.00 | 300.58 | 5.37 | 362.00 | 361.78 | 5.37 | 362.00 | 361.78 | 5.37 | 362.00 | 361.78 |
| 48.81 | 302.00 | 301.58 | 5.21 | 363.00 | 362.79 | 5.21 | 363.00 | 362.79 | 5.21 | 363.00 | 362.79 |
| 46.79 | 303.00 | 302.58 | 5.05 | 364.00 | 363.79 | 5.05 | 364.00 | 363.79 | 5.05 | 364.00 | 363.79 |
| 44.86 | 304.00 | 303.59 | 4.90 | 365.00 | 364.79 | 4.90 | 365.00 | 364.79 | 4.90 | 365.00 | 364.79 |
| 43.02 | 305.00 | 304.59 | 4.75 | 366.00 | 365.80 | 4.75 | 366.00 | 365.80 | 4.75 | 366.00 | 365.80 |
| 41.27 | 306.00 | 305.59 | 4.61 | 367.00 | 366.80 | 4.61 | 367.00 | 366.80 | 4.61 | 367.00 | 366.80 |
| 39.59 | 307.00 | 306.60 | 4.47 | 368.00 | 367.80 | 4.47 | 368.00 | 367.80 | 4.47 | 368.00 | 367.80 |
| 37.99 | 308.00 | 307.60 | 4.34 | 369.00 | 368.81 | 4.34 | 369.00 | 368.81 | 4.34 | 369.00 | 368.81 |
| 36.46 | 309.00 | 308.60 | 4.21 | 370.00 | 369.81 | 4.21 | 370.00 | 369.81 | 4.21 | 370.00 | 369.81 |
| 35.00 | 310.00 | 309.61 | 4.09 | 371.00 | 370.81 | 4.09 | 371.00 | 370.81 | 4.09 | 371.00 | 370.81 |
| 33.61 | 311.00 | 310.61 | 3.97 | 372.00 | 371.82 | 3.97 | 372.00 | 371.82 | 3.97 | 372.00 | 371.82 |
| 32.27 | 312.00 | 311.61 | 3.86 | 373.00 | 372.82 | 3.86 | 373.00 | 372.82 | 3.86 | 373.00 | 372.82 |
| 31.00 | 313.00 | 312.62 | 3.75 | 374.00 | 373.82 | 3.75 | 374.00 | 373.82 | 3.75 | 374.00 | 373.82 |
| 29.78 | 314.00 | 313.62 | 3.64 | 375.00 | 374.83 | 3.64 | 375.00 | 374.83 | 3.64 | 375.00 | 374.83 |
| 28.61 | 315.00 | 314.62 | 3.54 | 376.00 | 375.83 | 3.54 | 376.00 | 375.83 | 3.54 | 376.00 | 375.83 |
| 27.50 | 316.00 | 315.63 | 3.44 | 377.00 | 376.83 | 3.44 | 377.00 | 376.83 | 3.44 | 377.00 | 376.83 |
| 26.43 | 317.00 | 316.63 | 3.34 | 378.00 | 377.84 | 3.34 | 378.00 | 377.84 | 3.34 | 378.00 | 377.84 |
| 25.41 | 318.00 | 317.63 | 3.25 | 379.00 | 378.84 | 3.25 | 379.00 | 378.84 | 3.25 | 379.00 | 378.84 |
| 24.44 | 319.00 | 318.64 | 3.16 | 380.00 | 379.84 | 3.16 | 380.00 | 379.84 | 3.16 | 380.00 | 379.84 |
| 23.50 | 320.00 | 319.64 | 3.08 | 381.00 | 380.85 | 3.08 | 381.00 | 380.85 | 3.08 | 381.00 | 380.85 |
| 22.61 | 321.00 | 320.64 | 3.00 | 382.00 | 381.85 | 3.00 | 382.00 | 381.85 | 3.00 | 382.00 | 381.85 |
| 21.75 | 322.00 | 321.65 | 2.92 | 383.00 | 382.85 | 2.92 | 383.00 | 382.85 | 2.92 | 383.00 | 382.85 |
| 20.93 | 323.00 | 322.65 | 2.84 | 384.00 | 383.86 | 2.84 | 384.00 | 383.86 | 2.84 | 384.00 | 383.86 |
| 20.14 | 324.00 | 323.65 | 2.76 | 385.00 | 384.86 | 2.76 | 385.00 | 384.86 | 2.76 | 385.00 | 384.86 |
| 19.39 | 325.00 | 324.66 | 2.69 | 386.00 | 385.86 | 2.69 | 386.00 | 385.86 | 2.69 | 386.00 | 385.86 |
| 18.67 | 326.00 | 325.66 | 2.62 | 387.00 | 386.87 | 2.62 | 387.00 | 386.87 | 2.62 | 387.00 | 386.87 |
| 17.98 | 327.00 | 326.66 | 2.55 | 388.00 | 387.87 | 2.55 | 388.00 | 387.87 | 2.55 | 388.00 | 387.87 |
| 17.31 | 328.00 | 327.67 | 2.49 | 389.00 | 388.87 | 2.49 | 389.00 | 388.87 | 2.49 | 389.00 | 388.87 |
| 16.68 | 329.00 | 328.67 | 2.43 | 390.00 | 389.88 | 2.43 | 390.00 | 389.88 | 2.43 | 390.00 | 389.88 |
| 16.07 | 330.00 | 329.67 | 2.36 | 391.00 | 390.88 | 2.36 | 391.00 | 390.88 | 2.36 | 391.00 | 390.88 |

NBS Test No. 534/221273
June 25, 1980

Table 3

| THERMISTOR VOLTAGE | | BLACKBODY RADIANCE TEMP. (KELVINS) | THERMISTOR VOLTAGE | | BLACKBODY RADIANCE TEMP. (KELVINS) |
|-----------------------|------------|---|-----------------------|------------|---|
| 1 (MV.) | 2 (MV.) | | 1 (MV.) | 2 (MV.) | |
| 187.84 | 219.81 | 269.47 | 13.19 | 15.48 | 338.68 |
| 178.13 | 207.76 | 278.48 | 12.71 | 14.92 | 331.68 |
| 169.00 | 197.16 | 271.48 | 12.25 | 14.38 | 332.68 |
| 160.45 | 187.24 | 272.48 | 11.81 | 13.87 | 333.69 |
| 152.38 | 177.87 | 273.49 | 11.38 | 13.37 | 334.69 |
| 144.81 | 169.07 | 274.49 | 10.98 | 12.90 | 335.69 |
| 137.65 | 160.75 | 275.49 | 10.59 | 12.44 | 336.70 |
| 130.93 | 152.94 | 276.50 | 10.22 | 12.01 | 337.70 |
| 124.57 | 145.54 | 277.50 | 9.86 | 11.58 | 338.70 |
| 118.59 | 138.57 | 278.50 | 9.51 | 11.18 | 339.71 |
| 112.92 | 131.98 | 279.51 | 9.18 | 10.79 | 340.71 |
| 107.57 | 125.74 | 280.51 | 8.87 | 10.42 | 341.71 |
| 102.49 | 119.83 | 281.51 | 8.56 | 10.06 | 342.72 |
| 97.72 | 114.27 | 282.52 | 8.27 | 9.72 | 343.72 |
| 93.19 | 108.99 | 283.52 | 7.99 | 9.39 | 344.72 |
| 88.90 | 103.98 | 284.52 | 7.72 | 9.07 | 345.73 |
| 84.82 | 99.23 | 285.53 | 7.46 | 8.77 | 346.73 |
| 80.98 | 94.74 | 286.53 | 7.21 | 8.48 | 347.73 |
| 77.31 | 90.47 | 287.53 | 6.97 | 8.19 | 348.74 |
| 73.85 | 86.43 | 288.54 | 6.73 | 7.92 | 349.74 |
| 70.56 | 82.59 | 289.54 | 6.51 | 7.66 | 350.74 |
| 67.43 | 78.93 | 290.54 | 6.30 | 7.41 | 351.75 |
| 64.45 | 75.45 | 291.55 | 6.09 | 7.17 | 352.75 |
| 61.64 | 72.17 | 292.55 | 5.89 | 6.94 | 353.76 |
| 58.95 | 69.02 | 293.55 | 5.70 | 6.72 | 354.76 |
| 56.40 | 66.05 | 294.56 | 5.52 | 6.50 | 355.76 |
| 53.98 | 63.21 | 295.56 | 5.34 | 6.29 | 356.77 |
| 51.67 | 60.51 | 296.56 | 5.18 | 6.10 | 357.77 |
| 49.47 | 57.94 | 297.57 | 5.01 | 5.90 | 358.77 |
| 47.37 | 55.49 | 298.57 | 4.85 | 5.72 | 359.78 |
| 45.37 | 53.16 | 299.57 | 4.70 | 5.54 | 360.78 |
| 43.47 | 50.93 | 300.58 | 4.56 | 5.37 | 361.78 |
| 41.66 | 48.81 | 301.58 | 4.42 | 5.21 | 362.79 |
| 39.93 | 46.79 | 302.58 | 4.28 | 5.05 | 363.79 |
| 38.28 | 44.86 | 303.59 | 4.15 | 4.90 | 364.79 |
| 36.71 | 43.02 | 304.59 | 4.03 | 4.75 | 365.80 |
| 35.21 | 41.27 | 305.59 | 3.90 | 4.61 | 366.80 |
| 33.78 | 39.59 | 306.60 | 3.79 | 4.47 | 367.80 |
| 32.41 | 37.99 | 307.60 | 3.68 | 4.34 | 368.81 |
| 31.10 | 36.46 | 308.60 | 3.57 | 4.21 | 369.81 |
| 29.85 | 35.00 | 309.61 | 3.46 | 4.09 | 370.81 |
| 28.66 | 33.61 | 310.61 | 3.36 | 3.97 | 371.82 |
| 27.52 | 32.27 | 311.61 | 3.26 | 3.86 | 372.82 |
| 26.43 | 31.00 | 312.62 | 3.17 | 3.75 | 373.82 |
| 25.39 | 29.78 | 313.62 | 3.08 | 3.64 | 374.83 |
| 24.40 | 28.61 | 314.62 | 2.99 | 3.54 | 375.83 |
| 23.45 | 27.50 | 315.63 | 2.91 | 3.44 | 376.83 |
| 22.54 | 26.43 | 316.63 | 2.83 | 3.34 | 377.84 |
| 21.66 | 25.41 | 317.63 | 2.75 | 3.25 | 378.84 |
| 20.83 | 24.44 | 318.64 | 2.67 | 3.16 | 379.84 |
| 20.03 | 23.50 | 319.64 | 2.60 | 3.08 | 380.85 |
| 19.27 | 22.61 | 320.64 | 2.53 | 3.00 | 381.85 |
| 18.54 | 21.75 | 321.65 | 2.46 | 2.92 | 382.85 |
| 17.83 | 20.93 | 322.65 | 2.40 | 2.84 | 383.86 |
| 17.16 | 20.14 | 323.65 | 2.33 | 2.76 | 384.86 |
| 16.52 | 19.39 | 324.66 | 2.27 | 2.69 | 385.86 |
| 15.91 | 18.67 | 325.66 | 2.21 | 2.62 | 386.87 |
| 15.31 | 17.98 | 326.66 | 2.15 | 2.55 | 387.87 |
| 14.75 | 17.31 | 327.67 | 2.10 | 2.49 | 388.87 |
| 14.20 | 16.68 | 328.67 | 2.04 | 2.43 | 389.88 |
| 13.68 | 16.07 | 329.67 | 1.99 | 2.36 | 390.88 |

NBS Test No. 534/221273
June 26, 1980

Table 4. Table of Uncertainties

| | PERCENT UNCERTAINTY |
|---|---------------------|
| 1. ABILITY TO MAKE ELECTRICAL POWER MATCH TO RADIANT HEATING | 0.6 |
| 2. EMISSIVITY CALCULATION | 0.12 |
| 3. POWER CORRECTION FOR HEATER CONNECTION LEADS (DETECTOR) | 0.3 |
| 4. VOLTAGE MEASUREMENTS (AT .02 VOLTS) | 0.01 |
| 5. SOLID ANGLE | |
| A. DUE TO APERTURE SEPARATION (25.49 CM) COOLDOWN CORRECTIONS | 0.9 |
| B. DUE TO DETECTOR AREA (1.033 CM ²) COOLDOWN CORRECTIONS | 0.2 |
| 6. SOURCE AREA (3.313 x 10 ⁻³ CM ²) COOLDOWN CORRECTIONS | 0.8 |
| 7. THERMAL EMF | 0.4 |
| 8. CURRENT MEASUREMENT | 0.001 |
| 9. ERROR DUE TO VIEWING MORE THAN SIMPLY THE BLACKBODY APERTURE | 0.01 |
| 10. DIFFRACTION EFFECTS (2.5 TO 3.5% DEPENDING UPON TEMPERATURE) | 0.7 |
| TOTAL UNCERTAINTY (QUADRATURE) | 1.6 |
| (SUM OF ABSOLUTE VALUES) | 4.0 |

NBS Test No. 534/221273
June 26, 1980

NOMENCLATURE

| | |
|----------------------------------|---|
| a | Distance from blackbody output aperture to radiometer |
| A_d | Area of detector element in the radiometer |
| A_o | Area of detector image projected on heated cavity opening |
| A_p | Area of blackbody output aperture |
| b | Distance from blackbody cavity opening to blackbody output aperture |
| D | Diameter of blackbody output aperture |
| d | Diameter of blackbody cavity opening |
| E'_{min} | Fractional reduction of total energy on radiometer element due to diffraction effects |
| e_T | Voltage drop across thermistor with 5 μ A of bias current. |
| P | Power reaching radiometer element |
| T | Blackbody cavity temperature |
| T_o | Temperature of output aperture mount |
| Ω_M | Solid angle of blackbody output aperture as viewed from cavity opening |
| σ | Stefan-Boltzmann constant |
| \bar{r} | Average of the bolometer system responsivity measurements |
| r_i | The i^{th} determination of the bolometer system responsivity |
| \bar{R} | True bolometer system responsivity |
| B | Bias error from the NBS calibration |
| $t_{\alpha/2}$ | Student's two-tailed t factor for the $(1 - \alpha)$ confidence interval |